NAVAL POSTGRADUATE SCHOOL
Monterey, California

THESIS

Probabilistic Reliability Modeling of Fatigue on the H-46 Tie Bar

by

John C. O'Connor

September 1994

Thesis Advisor: Edward M. Wu

Approved for public release: distribution is unlimited

Unclassified
ECURITY CLASSIFICATION OF THIS PAGE

REPORT DOCUMENTATION PAGE

Form Approved
OMB No. 0704-0188

a. REPORT SECURITY CLASSIFICATION
Unclassified

1b. RESTRICTIVE MARKINGS

a. SECURITY CLASSIFICATION AUTHORITY

3. DISTRIBUTION/AVAILABILITY OF REPORT
Approved for public release: distribution is unlimited

b. DECLASSIFICATION/DOWNGRADING SCHEDULE

. PERFORMING ORGANIZATION REPORT NUMBER(S)

5. MONITORING ORGANIZATION REPORT NUMBER(S)

a. NAME OF PERFORMING ORGANIZATION
Naval Postgraduate School

6b. OFFICE SYMBOL (If applicable)

7a. NAME OF MONITORING ORGANIZATION
Naval Postgraduate School

c. ADDRESS (City, State, and ZIP Code)
Monterey, CA 93943-5000

7b. ADDRESS (City, State, and ZIP Code)
Monterey, CA 93943-5000

a. NAME OF FUNDING/SPONSORING ORGANIZATION

8b. OFFICE SYMBOL (If applicable)

9. PROCUREMENT INSTRUMENT IDENTIFICATION NUMBER

c. ADDRESS (City, State, and ZIP Code)

10. SOURCE OF FUNDING NUMBERS

PROGRAM ELEMENT NO.	PROJECT NO.	TASK NO.	WORK UNIT ACCESSION NO.

1. TITLE (Include Security Classification)
Probabilistic Reliability Modeling of Fatigue on the H-46 Tie Bar

2. PERSONAL AUTHOR(S)
John Charles O'Connor

13a. TYPE OF REPORT	13b. TIME COVERED	14. DATE OF REPORT (Year,Month,Day)	15. PAGE COUNT
Master's Thesis	FROM TO	September 1994	85

6. SUPPLEMENTARY NOTATION
The views expressed in this thesis are those of the author and do not reflect the official policy or position of the Department of Defense or the U.S. Government.

17. COSATI CODES			18. SUBJECT TERMS (Continue on reverse if necessary and identify by block number)
FIELD	GROUP	SUB-GROUP	Fatigue life, Probabilistic Fatigue Modeling

The H-46 helicopter has experienced early in-service failures in its tie bar. The tie bar is a multi-component system that is a critical part of the linkage, which attaches the rotor blade to the rotating hub of the helicopter. This research developed methodology to predict the life of the tie bar under nominal operational flight loads. A probability model is indispensable because a revised design has yet to accumulate field data, and laboratory testing can never be sufficiently extensive for non-parametric reliability prediction. An algorithm was developed for three and four component systems that will generate the probability of system failure based on the probability of failure in its components. Finite element analysis was conducted on the tie bar to determine stress on each component for all possible damage configurations of the tie bar. A given set of flight loads was resolved into boundary conditions for the stress analysis. A methodology was developed to determine the probability of failure of each component using an idealized load history, based on the expected stress-life (S-N) relation of the component at the stress levels experienced by the component. The result is a prediction method that can fortify laboratory results to predict the probability of failure of a system given the system load history. This model will be verified using the early in-service failure statistics of the current design and can be used to assess revised designs. The model will provide a prediction of the failure distributions, (the bell-shaped distribution) as a function of flight hours, for one, two, three, and four elements of failures within the leaves of the tie bar.

20. DISTRIBUTION/AVAILABILITY OF ABSTRACT
[X] UNCLASSIFIED/UNLIMITED [ ] SAME AS RPT. [ ] DTIC USERS

21. ABSTRACT SECURITY CLASSIFICATION
Unclassified

22a. NAME OF RESPONSIBLE INDIVIDUAL
Prof. Edward M Wu, Ph.D.

22b. TELEPHONE (Include Area Code)
(408) 656-3459

22c. OFFICE SYMBOL
AA/Wu

DD Form 1473, JUN 86
Previous editions are obsolete.
S/N 0102-LF-014-6603

SECURITY CLASSIFICATION OF THIS PAGE
Unclassified

Approved for public release: distributuion is unlimited

Probabilistic Reliability Modeling of Fatigue on the H-46 Tie Bar

by

John Charles O'Connor
Commander, United States Navy
B.S., University of Illinois, 1980

Submitted in partial fulfillment of the
requirements of the degree of

MASTERS OF SCIENCE IN AERONAUTICAL ENGINEERING

from the

NAVAL POSTGRADUATE SCHOOL
September 1994

Author: _____
John Charles O'Connor

Approved By: _____
Edward M. Wu, Thesis Advisor

_____
Gerald H. Lindsey, Second Reader

_____
Daniel J. Collins, Chairman, Department of Aeronautical and
Astronautical Engineering

ABSTRACT

The H-46 helicopter has experienced early in-service failures in its tie bar. The tie bar is a multi-component system that is a critical part of the linkage, which attaches the rotor blade to the rotating hub of the helicopter. This research developed methodology to predict the life of the tie bar under nominal operational flight loads. A probability model is indispensable because a revised design has yet to accumulate field data, and laboratory testing can never be sufficiently extensive for non-parametric reliability prediction. An algorithm was developed for three and four component systems that will generate the probability of system failure based on the probability of failure in its components. Finite element analysis was conducted on the tie bar to determine stress on each component for all possible damage configurations of the tie bar. A given set of flight loads was resolved into boundary conditions for the stress analysis. A methodology was developed to determine the probability of failure of each component using an idealized load history, based on the expected stress-life (S-N) relation of the component at the stress levels experienced by the component. The result is a prediction method that can fortify laboratory results to predict the probability of failure of a system given the system load history. This model will be verified using the early in-service failure statistics of the current design and can be used to assess revised designs. The model will provide a prediction of the failure distributions, (the bell-shaped distribution) as a function of flight hours, for one, two, three, and four elements of failures within the leaves of the tie bar.

TABLE OF CONTENTS

ACKNOWLEDGMENTS

I would like to mention and offer my warm appreciation to all the people whose time, effort and patience made this project a better work.

First, I would like to thank my wife Nicole whose belief in me and acceptance of my challenges as a shared challenge make my walk through life a little easier.

I would like to thank the engineer's at Naval Aviation Depot Cherry Point, NC, especially Mr. Robby Taylor whose assistance was always professional and immediate.

I would like to thank Prof. Gerald Lindsey who offered his time in the development of this paper.

Lastly, but most importantly, I would like to thank Dr. Edward Wu whose untiring patience and personal dedication to my real education left an everlasting impression. Thanks for teaching me how to fish!

I. INTRODUCTION

A. INTRODUCTION

The H-46 helicopter will be required to satisfy the Navy and Marine Corps mission requirements for the foreseeable future. Service life extension of the aircraft is dependent upon valid analysis of the useful life of the aircraft's components.

The H-46 tie bar is part of the linkage that attaches the helicopter's rotor blade to the rotating hub of the helicopter. The tie bar is a safety of flight component, and failure of one tie bar would result in the catastrophic loss of the aircraft. The original fatigue analysis has not adequately predicted the useful life of the component.

Early failure of the tie bar has already resulted in two aircraft mishaps. The Navy must inspect an aircraft every 10 hours using a fiber optic scope to check for broken straps in the tie bar. This heightened inspection cycle is needed for safety but adversely impacts mission readiness and aircraft availability.

Three alternative tie bar designs have been proposed to satisfy the replacement requirement when the present supply is depleted. One is geometrically similar to the present tie bar with minor changes in geometry to reduce stress concentrations, and it is chemically polished to remove manufacturing defects. The two others, a composite design and a steel wire design are significantly different.

The accepted design will have to eliminate the requirement for 10 hour inspections while providing improved cycle life and fail-safe performance.

The tie bar's fatigue crack initiation appeared to be random. Laboratory fatigue tests were conducted on the original tie bar design, and the results were used to model the fatigue life for all produced tie bars. The model failed to adequately predict the life of the tie bar.

Field data of the damaged tie bars exists. The contractor that manufactures the H-46, Boeing Helicopter, has proposed a series of fatigue tests to determine the reliability of the replacement tie bar design. The test is designed to replicate the loads, and load cycles experienced by the tie bar in nominal mission operation. The objective of the revised design is to improve the reliability of the tie bar at a reduced inspection interval.

Prior to production, reliability prediction of the revised design can be statistically based or probability based. In a statistically based approach, direct laboratory testing data is needed. For a moderate reliability level, $(1\text{-}10^{3})$ approximately 10^{4} testing articles are needed; an intractable task. In the probability based approach, the physical failure modes of the components (the individual leaves of the tie bar) are modeled by analytical logic leading to a functional representation of the system (the tie bar as a whole). Through a realistic probability model, the number of tests are reduced by several orders of magnitude. for the same comparable level of confidence in prediction.

The probability based approach adopted in this investigation will be verified by early in-service failure statistics. It will then be used to fortify limited laboratory testing, which is necessitated by constraints in resources and time.

B. RELIABILITY DETERMINATION

Reliability is a defined level of non-failure under a given set of operational conditions. Reliability information is critical in determining the safe life of systems and their components. Reliability information can be used to set inspection cycles or to determine provisioning requirements for replacement parts. The information can also be used to compare the reliability of design candidates or to evaluate the reliability improvement in a modification of the existing design.

1. Direct Testing vs. Analytical Modeling

Reliability can be estimated by statistical analysis of direct testing data or by system modeling.

Direct testing of aircraft components is usually impractical because the number of samples required to produce an accurate reliability estimate with a reasonable degree of certainty is an order of magnitude greater than the desired reliability. The desired reliability for a military aircraft is one failure in 100000 (or $1\text{-}10^5 = 0.99999$), therefore at least a million samples would have to be tested; an obvious impossibility.

Analytical modeling allows one to determine the probability with limited data or samples. The probabilistic model can be based on either experience, understanding of the physical phenomena, or a combination of both. Analytical models are created by identifying the salient physical process and then mathematically modeling the physics.

The fatigue processes of homogeneous metal has a very large data base. The relationship between the application of stress (S) and number of cycles (N) to onset of fatigue failure (the S-N curve) has been extensively modeled both empirically and analytically.

In this investigation, the traditional S-N fatigue relation is used to predict the individual component life (the straps of the tie bar). Probability modeling is explored to relate the combinatorial failure sequences of the components to predict the system life (the entire tie bar).

C. SCOPE OF THIS RESEARCH

The scope of this thesis was to develop a method for predicting the reliability of the H-46 tie bar. An algorithm was developed that would generate the probability of failure of a multi-component system from the probabilities of failure of its individual components. The probability of failure of each component was a function of the magnitude and duration

of cyclic stress experienced by the respective component. Stress analysis was conducted on the tie bar for an idealized flight load block representative of flight loads experienced during a nominal operational flight. Analysis of the kinematics of the rotor system during flight was used to correctly apply the flight load block parameters to the tie bar for computation of internal stresses within the components. A methodology was developed to use historical fatigue data and to verify and reconcile this model with the actual flight load block. A cumulative damage model is required in order to convolute the effects of different stress levels resulting from a varying load history (the flight load block). The stress on each component was determined by the finite element analysis for each load set in the flight load block. The model and the damage convolution allows the calculation of probability of failure of each component given the magnitude of the stress and the duration. The model will provide a prediction of the failure distributions, (the bell-shaped distribution) as a function of flight hours, for one, two, three, and four elements of failures within the leaves of the tie bar.

II. BACKGROUND

A. INTRODUCTION

Creating a reliability model required partitioning the analysis into three separate analyses; probability analysis, stress analysis, and fatigue analysis. The probability analysis developed an algorithm for calculating the failure probability of a multi-component system based on its components. The probability was a function of applied stress which was dependent on the geometric configuration of the system. Finite element stress analysis was conducted to obtain the stress for a given set of applied boundary conditions, the flight load block, and the different geometric failure configurations. A fatigue analysis methodology was developed to obtain a relationship between the strength of the system, the life of the system, and the magnitude and duration of cyclic stresses applied to the system.

B. PROBABILITY ANALYSIS

1. Probability Analysis of Physical Events

The failure of any of the components of the tie bar is a physical event. The number of components that have failed defines the physical configuration of the tie bar. An example is shown in Figure 1.

The tie bar leaf in (a) is whole, none of the components have failed. The tie bar leaf in (b) has experienced a failure of component A. The physical configuration of the tie bar has changed. As the physical configuration of the system changes, so do the internal stresses and the probability of failure of the remaining components and thus the system.

2. Failure Sequence

The overall reliability of the system depends on the initial state, or configuration, of the system and the final state of the entire system. Applying this concept to the tie bar, the

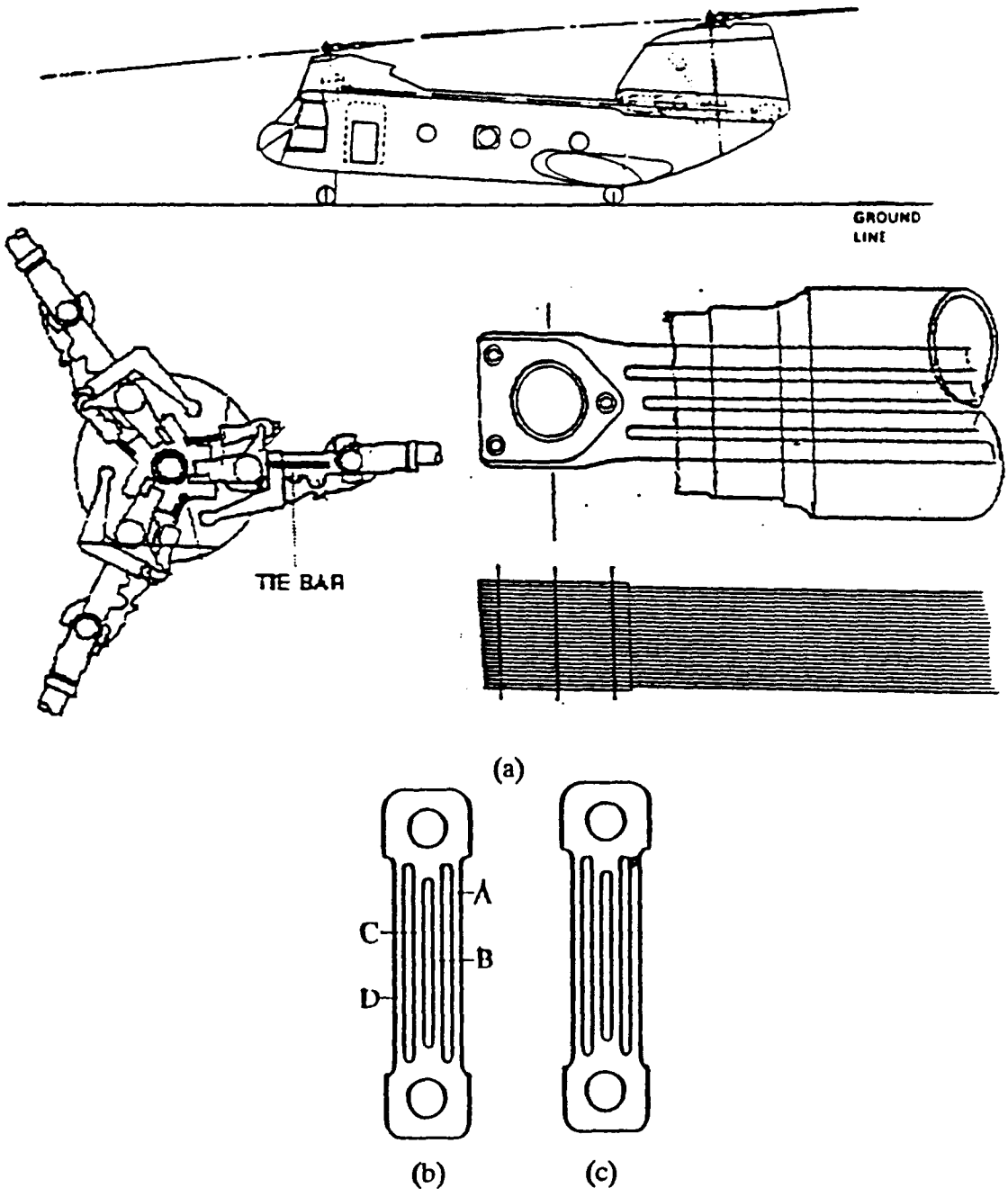

Figure 1. (a) Overall Perspective of Location of Tie Bar in Helicopter

(b) Undamaged Tie Bar Straps A through D

(c) Damaged Tie Bar on strap A

probability of three straps of a tie bar failing during a flight is dependent on whether zero, one, or two had failed prior to and during the flight.

This concept is depicted graphically in Figure 2 for a motivating example of a three component system (Say a tie bar with three straps). For a three component system, there are eight possible configurations, depending on the relative strength of the components. The first transition is from a state of no failures to a state of one, two, or three failures.

A second transition occurs from states where one failed or two have failed. The probability that one branch of the failure tree is followed to failure is different than the probability of the occurrence of the other branches.

In the case of this three strap tie bar leaf, the global loads on the tie bar remain unchanged (as dictated by the flight condition) and the local stress in each component (strap) changes as a function of the configuration; i.e., the number of failed straps on the tie bar leaf. The tie bar can be observed as a system with three components each with a different strength relative to the other two components. For the tie bar which is loaded so that each component experiences the same stress, the first component to fail is the weakest of the three. If two break simultaneously, they have the same strength and are weaker than the last to fail.

In characterizing the strength of the tie bar strap, the local stress experienced by each individual strap is the random variable (RV) and the strength of each strap, in this case, the value at which it fails, is the realized random variable (RRV).

3. Physical Events to Probability

The fatigue failure of the component is envisioned to be caused by growth of pre-existing flaws in the component. The statistical distribution of the severity and spatial location of such flaws determines its failure characteristics. Catastrophic failure occurs when the stress at any one flaw exceeds the ability of the surrounding material to halt crack

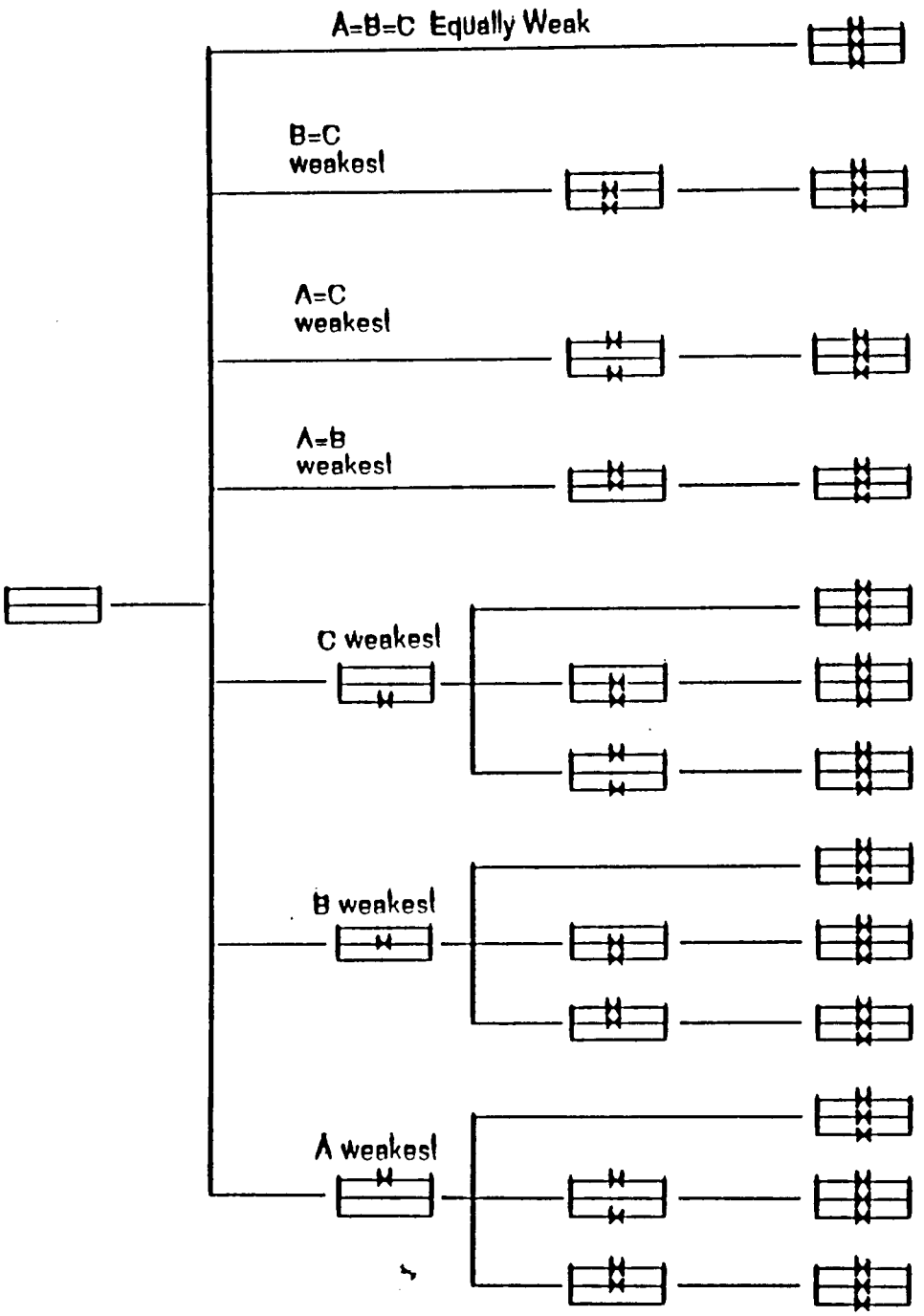

Figure 2. Three Component Failure Tree

propagation. This local failure leads to the global failure of the entire system, which consists of many components; hence, the weakest link of the chain visualization. Weibull derived the following expression to describe the weakest link distribution:

$$F(x)=1-\exp\{-(x/\beta)^{\alpha}\}$$

where

$F(x)$ = the probability of failure of the component under stress x

x = the applied stress

β = a scale parameter

α = a shape parameter

Applying this to the tie bar:

$$F_{A|i}[x_A(L)] = 1-\exp\{-(x_A(L)/\beta)^{\alpha}\}$$

where

$F_{A|i}[x_A(L)]$ = the probability of failure of component A (a strap) under stress x_A in the i^{th} configuration (one, two, or three strap failures).

$x_A(L)$ = the applied stress on component A caused by the global load L

β = a scale parameter of the material strength

α = a shape parameter of the material variability

The local stress experienced by each component can be calculated for each configuration (eight total in a three component system, Figure 2) but the relative strengths cannot be determined unless the failure path which lead to that configuration is known.

Chapter III defines an algorithm to calculate the probability of failure of a system (the tie bar leaf) given the initial configuration; zero, one, two, or three failed and the final configuration one, two, three, or all failed. The algorithm is initially defined for a system with three components and then extended to a system with four components. The algorithm uses the probability of failure of the individual components to arrive at the probability of failure of the entire system.

C. STRESS ANALYSIS

Most modern aircraft structures are highly complex assemblages of many individual parts. If a structure is broken down into its basic parts, one can idealize each part and apply any appropriate analysis method, such as shear flow, torsion or beam bending theory to solve for stresses and displacements.

The field equations of a solid continuum describe the relationship between forces, displacements, stresses, and strains of a structure. There are 15 coupled partial differential equations in 15 unknowns.

The field equations are summarized below:

$$T_i = \sigma_{ji} \nu_j$$

$$\partial_i \sigma_{ij} + X_j = 0$$

$$\varepsilon_{ij} = \frac{1}{2}(\partial_i u_j + \partial_j u_i) + \frac{1}{2}(\partial_i u_k \times \partial_j u_k)$$

$$\sigma_{ij} = C_{ijkl} \varepsilon_{kl}$$

for i,j,k,l = 1,2,3

where:

T = surface traction vector
σ = stress
ν = outward normal vector
X = body force
ε = strain
u = displacement
C = material constant

Simple structures are statically determinate. That is, the equilibrium equations are sufficient to determine the internal force resultants necessary to obtain stresses, strains, and deformations.

The analysis of structures increases in difficulty with the complexity of the structure. Most aircraft structures are statically indeterminate, and all the field equations remain

coupled and are difficult to solve. When the structure reaches a complexity such that the additional deformation equations are hard to establish, more general techniques are used. The techniques define equilibrium in terms of work and energy. Work and energy are defined in terms of both force and displacement so that the essential equilibrium and compatibility are combined in the techniques. Work and energy based techniques are path independent, that is, they define static equilibrium in terms of the scalar quantity, energy. Thus, the techniques can be applied to indeterminate structures where an exact solution or an idealized solution technique is impractical. Specifically, the finite element stiffness method is used. [Ref. 1:p. 399]

The concept of the finite element stiffness method is to view the complete structure as an assemblage of a finite number of discrete elements. Each element's deformation response is pre-computed relative to the response of the complete structure. The complete structure is broken down into elements, each element is analyzed separately for equilibrium, and the structure is reassembled by invoking compatibility requirements for displacements and equilibrium requirements for forces where the elements are connected. The assemblage uses the principles of work and energy to establish equilibrium. The finite element method is a stiffness method. That is, the displacements are considered independent variables.

Chapter IV applies the finite element analysis to one leaf of the tie bar to obtain the stresses on each component (strap) for every possible failure configuration.

D. FATIGUE ANALYSIS

1. Methods

Metal fatigue is a process in which a component fails after subjected to repeated loading. Because fatigue is difficult to quantitatively describe and model on the microscopic level, empirical fatigue analysis methods have been developed to allow one to

design against fatigue damage. Three primary fatigue analysis methods are used in engineering analysis. These are the stress-life approach, the strain-life approach, and the fracture mechanics approach. [Ref. 2:p. 232-235]

2. Stress-Life Approach

The stress-life approach works very well for analyzing structures subjected to relatively constant amplitude loading and stress levels in the elastic range. The method is basically empirical and does not model the mechanisms of fatigue. The method works well when used with insights offered by the other methods.

The empirical relationships are based on test data of steels in the intermediate to long life region. Care must be taken when extrapolating these relationships beyond the range of data used to determine them. When dealing with a new, or unique, set of conditions such as a new material or a unique type of loading, a new set of tests should be run and empirical relationships determined for that set of data.

The basis of the stress-life method is the plot of alternating stress, S, versus cycles to failure, N. A frequently used basic test is the rotating beam test in which the loading procedure produces a fully reversed uniaxial state of stress. One of the major assumptions of the stress-life approach is that it does not account for true stress-strain behavior and treats all strains as elastic. This assumption is valid only if the plastic strains are small. This condition is important since many initiations of fatigue cracks are caused by plastic deformation. The stress test data are usually presented on a log-log plot called an S-N curve. The line on the S-N curve represents a model of the data.

Most body-centered cubic steels have an endurance limit, σ_e, which is the stress below which the life of the material is greater than a million cycles and defined as infinite. The endurance limit may not exist if the specimen is exposed to periodic overloads, corrosive environments, or high temperatures.

An important aspect of fatigue data representation is that only sets of data from identical load histories can be pooled, i.e., data from different load histories form different S-N curves. For *constant* amplitude cyclic loading, interaction relations are used to interpolate life prediction under different minimum and maximum stresses. This method is discussed in the following section. For no constant amplitude cyclic loading, additional formulation on cumulative damage will be discussed in Chapter V.

3. Stress Ratio Transformation

The most common fatigue tests conducted are those applying a constant amplitude, fully reversed stress, that is, a load history such that the load alternates about a mean stress of zero. If data is collected for mean stresses that are not zero, a stress ratio is defined. The stress ratio is the ratio of the minimum stress to the maximum stress:

$$R = \frac{\sigma_{min}}{\sigma_{max}}$$

Two other stresses are also defined. The stress amplitude σ_a, where:

$$\sigma_a = \frac{\sigma_{max} - \sigma_{min}}{2}$$

and the mean stress σ_m, where:

$$\sigma_m = \frac{\sigma_{max} + \sigma_{min}}{2}$$

Stresses can be mapped into the zero mean stress domain or domain where the model was established using one of several empirical interaction relationships. The methods relate the mean stress and stress amplitude to the endurance limit to either the yield strength, ultimate strength, or true fracture stress of the material. The method can be generalized to be of the form:

$$\left(\frac{\sigma_a}{\sigma_e}\right)^k + \left(\frac{\sigma_m}{\sigma_{ult}}\right)^j = 1$$

where

σ_e= endurance limit stress

σ_{ult}= the ultimate stress

k,j = arbitrary constants

For the Goodman form, k=1, j=1; for the Soderberg form, k=2, j=1. [Ref. 2:p. 7-10].

In the operational environment of a helicopter, the tie bar experiences a load history of different stress ratios. The fatigue life prediction method is explained in Chapter V.

4. Cumulative Damage

Accumulation of the effect of the hazard on the specimen over time is of convolution form. The applied stress, which is a function of time, causes damage. The method by which stress increases damage is called the breakdown rule. The breakdown rule is convoluted over time. The damage caused by one multiple load history is integrated over the time for which the loads were applied. Damage may be integrated linearly or non-linearly. The linear damage rule, or Miner's rule states that the fraction of damage at a given stress level is equal to the number of cycles experienced at that stress level divided by the fatigue life in cycles at that stress level. The damage fractions are added to obtain the total damage fraction or percentage of life used. This is a linear convolution of a breakdown rule.

Chapter VI describes a methodology by which the convolution of the damage breakdown rule can be tested for linearity.

III. PROBABILITY ANALYSIS

This chapter develops the algorithm for determining the probability of failure of a system with multiple components in terms of the probability of failure of its components. The previous chapter briefly described the role of failure sequence of the components in determining the failure of a multi-component system. More explicitly, the failure sequence is determined by the relative strength (RRV) of each component relative to the other components in the system for the stress(RV) experienced by the component in a specific geometric configuration. Thus, the probability of failure of a specific system is dependent on the combinations of relative strength of its components.

A. NOTATION

1. Component Notation

Components are denoted by a capital letter. A component which has failed is denoted by an underlined capital letter.

2. Indicator Function

An indicator function was established in order to establish an algorithm for the states of a component of a system. For one of the components in the system:

$$I_S(x) = \begin{cases} 1 \text{ if } x \text{ is in } S \\ 0 \text{ if } x \text{ is not in } S \end{cases}$$

where S is a set of {attributes}; e.g., weight, straps over 40 grams; color, brown from heat treatment, or {conditions}, e.g., refurbished after 100 hr., electro-polished, or {events}, e.g. fail up to yield stress, as measured (RV) by x. Attributes and conditions can be discrete and do not result in the transition of a system. They are generally described by a

probability density function (pdf). Events are a measurement of, or the realization of, a transition. The transition occurs at but not before a certain value of the RV. The probability of a transition is usually described by a cumulative density function (CDF).

For example, S represents the strength (broken or not) of all possible elements at location A of a leaf and x is the applied stress at location A for a specific geometric configuration of the leaf. The Venn diagram representation for x is a line (a one-dimensional region) and x_A occupies a portion of this line.

Multiple components of a system define the condition but the indicator function focuses only on one component.

$X_S(x) \blacksquare I_S(x)$

For example, if a system is loaded such that component A experiences x, and only those systems where B and C have not failed are collected, $I(x_A, B, C) = 0$ or 1 depending on whether A has failed or has not failed.

If there are a total of three components in a system, one indicator function is needed for each of the three components for a total of three.

3. Geometric States

The number of possible states encompasses combinations of components that have failed and components that have not failed; combinatorial states. $\underline{A}B$ means $\underline{A} \cup B$, stated as A has not failed or B has failed or both A has failed and B has not failed. The probability of A B can be expressed as $R_A(x_A)F_B(x_B)$ or the reliability of A up to the value x_A multiplied by the probability of failure of B at the value x_B given that the underlying probability of failures of A and B are independent.

The transition of states involves permutations which describe the order or arrangement of the transitions, i.e., $AB \rightarrow A\underline{B}$ and $AB \rightarrow \underline{A}B$. Transition of states requires application of the concept of transitional probability. In the case $AB \rightarrow A\underline{B}$, the probability of the transition, which is the cumulative density function (CDF), can be

expressed as $R_A(x_A)R_B(x_B) - R_A(x_A)F_B(x_B)$. Stated in words, the probability that A did not fail at the value x_A and the probability that B did not fail at x_B, minus the probability that A did not fail at x_A and B failed at x_B.

The permutations are the branches of the failure tree. Every progressive step along each permutation needs conditional states. The cause of the transition is the stress state or stress history.

4. Conversion from Sets to Probability

The conversion from set theory to probability theory is made below:

$A \cap B$;	Intersection, Both A and B
$A \cup B$;	Union, Either A or B or both A and B
$P\{A \cap B\} = P\{A\|B\}P\{B\}$	3rd Axiom of Probability Theory

The third Axiom states in words that the probability of observing *both* A *and* B is equal to the probability of observing A from the sub-population containing B, multiplied by the probability of observing B from the original population. [Ref. 3:p. 10-16]

If A is independent of B, this is stated as the probability of observing A from a sub-population containing B is the same as that of observing A from the original population This interpretation is obvious for states and attributes (pdf). Events are independent if the probability of one event occurring is not dependent on the fact that another event is occurring or not occurring [Ref. 3:p. 12]. Thus:

$P\{A\|B\} = P\{A\}$	with the random variables (RV) explicitly expressed
$P\{A(x_A)\|B(x_B)\} = P\{A(x_A)\}$	for independent events

For independent events, the probability of observing A (not failed under load x_A i.e., up to and including (uti)x_A) from the subset which includes only components with conditions B (not failed up to and including load x_B) has the same probability of observing A (not failed uti load x_A) from the population which includes both components with conditions B (not failed under x_B) and $\underline{B}$ (failed under x_B). This means that the transition B to $\underline{B}$ may change the load in A from x_A to x'_A, thereby changing the probability of

observing A from $P\{A(x_A)\}$ to $P\{A(x'_A)\}$, but the probability of observing A at the original load x_A remain the same. The geometric configuration dependence is accounted for by the respective loads x_A, x_B from stress analysis.

5. Representing Probability by Functions

The notion of independence can be clarified when the probabilities are represented by functions. The functions are denoted:

$f_A(x_i) = P\{A(X = x_i)\}$

$F_A(x_i) = P\{A(X \le x_i)\}$

$f_{A|B}(x_i) = P\{A(X = x_i) \mid B\}$

$F_{A|B}(x_i) = P\{A(X \le x_i) \mid B\}$

In general, $f_{A|B} \neq f_A$, and $F_A \neq F_{A|B}$ i.e., the two functions are different, or parameters of the two functions are different.

6. Summary

A summary of probability axioms applied to systems of two, three, and four components are summarized below.

$P\{A\cap B\} = P\{A|B\}P\{B\}$ 3rd Axiom of Probability Theory (1)

$P\{A\cap B\} = P\{A\}P\{B\}$ A is independent of B (2)

$P\{A\cap B\} = 0$ A and B are mutually exclusive (3)

$P\{A\cup B\} = P\{A\} + P\{B\} - P\{A\cap B\}$ (4)

$P\{A\cup B\} = P\{A\} + P\{B\} - P\{A\}P\{B\}$; A is independent of B (5)

$P\{A\cup B\} = P\{A\} + P\{B\};$ A and B are exclusive (6)

$$P\{A\cup B\cup C\}=P\{A\}+P\{B\}+P\{C\}-P\{A\cap B\} -P\{B\cap C\} -P\{A\cap C\}+ +P\{A\cap B\cap C\} \quad (7)$$

$$P\{A\cap B\cap C\} = P\{A|B\cap C\}P\{B\cap C\}=P\{A|B\cap C\}P\{B|C\}P\{C\} \quad (8)$$

Applied to four components the equations (7) and (8) become:

$$P\{A\cup B\cup C\cup D\} = P\{A\}+P\{B\}+P\{C\}+P\{D\}- -P\{A\cap B\} -P\{B\cap C\} -P\{A\cap C\}-P\{A\cap D\}- -P\{B\cap D\} -P\{C\cap D\} +P\{A\cap B\cap C\cap D\} \quad (9)$$

$$P\{A\cap B\cap C\cap D\} = P\{A|B\cap C\cap D\}P\{B\cap C\cap D\}= = P\{A|B\cap C\cap D\}P\{B|C\cap D\}P\{C|D\}P\{D\} \quad (10)$$

B. CONSTRUCTING AN ALGORITHM

1. Formulation

The following is the formulation of an algorithm for three components whose intrinsic strength is independent; the intrinsic strength of each component is not effected by the failure of one of the other components.

The geometric states for the first component are either not failed A, or failed $\underline{A}$.

The symbol p_A represents the probability of observing A not failed when subjected to load up to x_A:

$$P\{A(x_A)\} = p_A$$

and p_A can be quantitatively estimated $F_A(A(x_A))$.

The symbol q_A represents the probability of observing A failed when subjected to load up to x_A:

$$P\{\underline{A}(x_A)\} = q_A$$

and q_A can be quantitatively estimated $1-F_A(A(x_A))$.

and

$$p_A + q_A = 1.$$

Similarly, the geometric states for the second components are either not failed B, or failed $\underline{B}$.

Thus p_B is the probability of observing B not failed when subjected to load up to x_B:

$$P\{B(x_B)\} = p_B$$

and q_B is the probability of observing B failed when subjected to load up to x_B:

$$P\{\underline{B}(x_B)\} = q_B$$

and

$$p_B + q_B = 1.$$

In general ,the geometric states for the second components are either not failed K, or failed $\underline{K}$.

The value p_k is the probability of observing K not failed when subjected to load up to x_K:

$$P\{K(x_k)\} = p_k$$

and q_K is the probability of observing K failed when subjected to load up to x_K:

$$P\{\underline{K}(x_K)\} = q_K$$

and

$$p_K + q_K = 1.$$

Consider the system of three components starting in an initial state of no failures that is both A, and B, and C. The probability of observing this state is:

$$P\{A(x_A) \cap B(x_B) \cap C(x_C)\} = P\{ABC\} = P\{A|B\cap C\}P\{B|C\}P\{C\} =$$
$$= P\{A\}P\{B\}P\{C\} \quad \text{by (8)}$$

The intrinsic strength is independent among the components so:

$$F_K = F_{K|J\,;\,k,j=A,B,C}\,(\text{CDF}) = p_A\, p_B\, p_C \qquad (11)$$

2. Casting Physical Problem in Terminology of Probability

The steps for casting the physical problem into probability formulation are established below; the physical reasoning for each individual step is elaborated on at the end of the development.

$$P\{\text{failure of system}\} = P\{\text{failure of all components}\} \qquad (12\text{-i})$$

$$P\{\text{failure of all components}\} = P\{\text{failure of all components} \cap \cap (\text{all failure sequences of components})\} \qquad (12\text{-ii})$$

$$P\{\text{failure of all components} \cap (\text{all failure sequences of components})\} = P\{\text{failure of all components} \cap (\cup \text{each failure sequence})\} \qquad (12\text{-iii})$$

$$P\{\text{failure of all components} \cap (\cup \text{each failure sequence})\} = P\{\cup (\text{failure of all components} \cap \text{each failure sequence})\} \qquad (12\text{-iv})$$

$$P\{\cup \text{(failure of all components « each failure sequence)}\}$$
$$= \sum_{\text{all sequences}} P\{\text{failure of all components} \cap \text{each failure sequence}\} \quad \text{(12-v)}$$

$$\sum_{\text{all sequences}} P\{\text{failure of all components} \cap \text{each failure sequence}\} \quad \text{(12-vi)}$$
$$= \sum_{\text{all sequences}} P\{\text{failure of all components} \mid \text{each failure sequence}\} P\{\text{each failure sequence}\}$$

$$\sum_{\text{all sequences}} P\{\text{failure of all components} \mid \text{each failure sequence}\} P\{\text{each failure sequence}\}$$
$$= \sum_{\textit{all sequences}} 1 \times P\{\text{each failure sequence}\} \quad \text{(12-vii)}$$

System failure is defined as the failure of all components (12-i) which is the failure of all components out of (intersection) all possible failure sequences of component combinations (each branch of the failure tree) (12-ii). In the case of a tie bar leaf, a combination is a geometric configuration. The arrangement of the combination in the sequence is dictated by admissibility. If a component has failed in the previous state, the only admissible component combinations after the transition are those with the same component failed. The system cannot repair itself. This implies mutual exclusivity.

By the distributive law, the failure of all components out of (intersect) all (union) failure sequences of the components which includes every branch of failure tree; (12-iii).

The Probability of failure of the total system reduces to the sum of the probability of each of the sequences by the law of total probability, (12), also known as Bayes' Theorem. [Ref. 4:p. 55-57]

Because P{failure of all components| each failure sequence} is the total probability it is equal to 1. The binomial formulation of p & q, inclusive and exclusive events' products, now becomes sums of inclusive events only.

$$= \sum_{\textit{all sequences}} P\{A \rightarrow \underline{A}\} \times P\{B \rightarrow \underline{B}\} \times P\{C \rightarrow \underline{C}\} \quad \text{(12)}$$

Therefore, the calculation of the probability of failure of a system of *n* independent components is the sum of the product of each of all the possible failure sequences of the components. The probability is computable from the respective CDF's.

3. Initial States

For a system of three components, there are a total $2^3 = 8$ possible combinatory states. These states can be represented in terms of the indicator function either in binary or octal format. TABLE 1 shows the possible initial states and their associated probabilities.

TABLE 1. PROBABILITY OF INITIAL STATES.

Octal Number	Initial States	Probability
7	111 CBA	$p_C p_B p_A$ (eqn 11)
6	110 CBA	$p_C p_B q_A$
5	101 CBA	$p_C q_B p_A$
4	100 CBA	$p_C q_B q_A$
3	011 CBA	$q_C p_B p_A$
2	010 CBA	$q_C p_B q_A$
1	001 CBA	$q_C q_B p_A$
0	000 CBA	$q_C q_B q_A$

Because they include all the possible states the sum of the probability is unity as previously stated by (12). To verify:

7 and 6 = $(p_A + q_A)\, p_B\, p_C$

5 and 4 = $(p_A + q_A)\, q_B\, p_C$

$p_B p_C + q_B p_C = (p_B + q_B) p_C = p_C$

3 and 2 = $(p_B + q_B)\, p_A q_C = p_A q_C$

1 and 0 = $(p_B + q_B)\, q_A q_C = q_A q_C$

$p_A q_C + q_A q_C = (p_A + q_A)\, q_C = q_C$

$(p_C + q_C) = 1$

4. Transition From the Initial State

The geometric configurations of the initial state determine the number of possible transitions leading to the second state. Given:

Initial State is 1 (none fail) there are $2^3 - 1 = 7$ transitions

Initial State is 2 or 3 or 4 (one fail) there are $2^{(3-1)} - 1 = 3$ transitions.

Initial State is 5 or 6 or 7 (two fail) there are $2^{(3-2)} - 1 = 1$ transitions.

Initial State is 8 (three fail) there are $2^{(3-3)} - 1 = 0$ transitions.

Consider the initial state of the system is 1 {CBA}. From one possible transition $\underline{A}$ (1st branch in diagram) the resulting second states and the associated probabilities are:

$P\{\underline{A}\} = P\{\underline{A} \cap (BC \cup \underline{B}C \cup B\underline{C} \cup \underline{BC})\}$ $\underline{A}$ out of all possible combinations of the remaining components; i.e. all outcomes within branch 1

$= P\{\underline{A}BC \cup \underline{AB}C \cup \underline{A}B\underline{C} \cup \underline{ABC})\}$ Distributive law

$= P\{\underline{A}BC\} + P\{\underline{AB}C\} + P\{\underline{A}B\underline{C}\} + P\{\underline{ABC}\} - P\{\underline{A}BC \cap \underline{AB}C\} - P\{\underline{A}BC \cap \underline{A}B\underline{C}\} -$
$- P\{\underline{AB}C \cap \underline{A}B\underline{C}\} + P\{\underline{A}BC \cap \underline{AB}C \cap \underline{A}B\underline{C} \cap \underline{ABC}\}$

$= P\{\underline{A}BC\} + P\{\underline{AB}C\} + P\{\underline{A}B\underline{C}\} + P\{\underline{ABC}\} - P\{\underline{A}BC \mid \underline{AB}C\}P\{\underline{AB}C\} -$
$- P\{\underline{A}BC \mid \underline{A}B\underline{C}\}P\{\underline{A}B\underline{C}\} - P\{\underline{A}B\underline{C} \mid \underline{ABC}\}P\{\underline{ABC}\} +$
$+ P\{\underline{A}BC \cap \underline{AB}C \cap \underline{A}B\underline{C} \cap \underline{ABC}\}$

$= P\{\underline{A}BC\} + P\{\underline{AB}C\} + P\{\underline{A}B\underline{C}\} + P\{\underline{ABC}\}$ by Independence

$= q_A p_B p_C + q_A q_B p_C + q_A p_B q_C + q_A q_B q_C$ by (11)

$= q_A p_C (p_B + q_B) + q_A q_C (p_B + q_B)$

$= q_A (p_C + q_C)$

$= q_A$ (13)

The probability of observing A fail (under a given RV) out of all the possible combinations of the remaining components (B,C) reduces to the probability of failure of A (under the given rv) by (13)

5. First Transition

The 7 possible transitions from the initial state {CBA}, as denoted by the first branchings of the failure tree and their associated probabilities are found in the similar manner and are listed in TABLE 2:

TABLE 2. TRANSITIONS FROM INITIAL STATE {CBA}

Code trnstn-branch	Possible 1st transition		Possible 2nd States	probability
1-1	A	6_8	CBA, CBA, CBA CBA	q_A
1-2	B	5_8	CBA, CBA, CBA, CBA	q_B
1-3	C	3_8	CBA, CBA CBA, CBA	q_C
1-4	BA	4_8	CBA, CBA	$q_B q_A$
1-5	CA	2_8	CBA, CBA	$q_C q_A$
1-6	CB	1_8	CBA, CBA	$q_C q_B$
1-7	CBA	0_8	CBA	$q_C q_B q_A$

6. Second Transition

Second transitions are defined as the possible states given the state after the first transition. Following the Boolean description of the appropriate states and specializing for independence of the intrinsic strength of the components, we can obtain all the second transitions with the possible ensuing states and the associated probabilities. TABLE 3 presents all the possible second transitions. TABLE 4 presents all possible third transitions.

C. QUANTIFYING PROBABILITY

1. Quantitative Determination of p_k and q_k

As stated previously, a quantitative value for the probability of failure of a component can be determined by defining a function that most accurately models the outcome of the random variable. There are two types of functions used in describing the

distribution of the random variable; the probability density function and the cumulative density function.

TABLE 3. POSSIBLE SECOND TRANSITIONS

First Trantn branch		Possible 2nd trantns	Possible states for 2nd states	Probability
1-1 A	1-1-1	B	ABC, ABC	q_B
	1-1-2	C	ABC, ABC	q_C
	1-1-3	BC	ABC	$q_B q_C$
1-2 B	1-2-1	A	ABC, ABC	q_A
	1-2-2	C	ABC, ABC	q_C
	1-2-3	AC	ABC	$q_A q_C$
1-3 C	1-3-1	A	ABC, ABC	q_C
	1-3-2	B	ABC, ABC	q_B
	1-3-3	AB	ABC	$q_A q_B$
1-4 AB	1-4-1	C	ABC	q_C
1-5 AC	1-5-1	B	ABC	q_B
1-6 BC	1-6-1	A	ABC	q_A

TABLE 4. POSSIBLE THIRD TRANSITIONS

Second Trantn branch		Possible 3rd trantns	Possible states for 3rd states	Probability
1-1-1 AB	1-1-1-1	C	ABC	q_C
1-1-2 AC	1-1-2-1	B	ABC	q_B
1-2-1	1-2-1-1	C	ABC	q_B
1-2-2	1-2-2-1	A	ABC	q_A
1-3-1	1-3-1-1	B	ABC	q_B
1-3-2	1-3-2-1	A	ABC	q_A

When A, B, and C are attributes, the respective p_k are probability *density* functions, f_k, evaluated at the RV x. In cases where A, B, and C are identical and independent(iid), $f_A = f_B = f_C$. When A, B, and C are events, the respective p_k are *cumulative* density functions, F_k, evaluated up to and including x. For iid, $F_A = F_B = F_C$.

In a system with multiple components, the random variable applied to the system is distributed to components by the characteristic process (for example boundary load is distributed to stresses in the internal elements following rules of the system of field equations).

The system random variable is denoted as the Global Random Variable (GRV), x. The random variable associated with the j^{th} component is denoted as the Local Random Variable (LRV), x_j.

The system configuration is denoted as {k} where k is an octal indicator of the combinatorial states of the components.

Under this notation, the probability of the failure event of the j^{th} up to and including the externally applied load L is:

$F(L \leq L \mid \{k\})$	Probability of failure of the System:
$F_{j\mid\{k\}}[x_j(L)\mid\{k\}]$	Probability of failure of component j dependent on {k}
$F_j[x_j(L)\mid\{k\}]$	Probability of failure of component j independent of {k}
$F[x(L)\mid\{k\}]$	Probability of failure if all components are iid

2. Generating Octal Indicators

Octal indicators are used to condense notation of combinatorial states. To convert binary indicator to octal indicator:

1. Number of combinations: 2^n; n = number of components
2. Highest octal number = 2^n-1
3. Highest octal state corresponds to undamaged configuration
4. Arrange binary indicators such that:
   a. the right column alternates, 1,0,1,0,1...every 2^0
   b. the next column alternates, 1,1,0,0,1,1...every 2^1
   c. 3rd column from the right alternates, 1,1,1,1,0,0,0,0,1...2^2
   d. nth column from the right, alternate every 2^{n-1}

3. Establishing the Algorithm

Consider the probability of failure of a three component system. The intrinsic strength of the components are independent. As a consequence, the probability of the failure of the j^{th} component reduces to q_j by (13).

On loading a system to load L, the probability of observing a sequence of transitions can be considered the formulation for the sequence 7640 (first branch of the failure tree along the first bifurcation), shown in TABLE 5.

TABLE 5. PROBABILITY FORMULATION FOR ONE SEQUENCE

State Indicator		Probability of Failure of Component $L \leq L$		
Binary	Octal	C	B	A
111	7			
110	6			$F_{A\|7}[x_{A\|7}(L)]$
100	4		$F_{B\|6}[x_{B\|6}(L)]$- $F_{B\|7}[x_{B\|7}(L)]$	
000	0	$F_{C\|4}[x_{C\|4}(L)]$- $F_{C\|6}[x_{C\|6}(L)]$		

Reasoning for filling the above table: The probability of failure of the state within all sequences reduces to just the probability of that state (by 11).

Examining the probability of each component for each combinatorial state, an algorithm can be seen:

A-7, observed by binary indicator that no break occurred, therefore q(A-7) = 0. In words, the CDF of component A subjected to the stress X_A for the physical configuration that B and C and A have not failed (state 7) subjected to loads up to L associated with RPM, flapping angle, and feathering angle, $x_{A|7}$ (L), is a function representation of Finite Element Analysis.

B-7, observed by binary indicator; no break, therefore q(B-7) = 0

C-7, observed by binary indicator; no break, therefore q(C-7) = 0

A-6, observed by binary indicator; a break, therefore calculate the probability of failure

before the transition and subtract the probability of failure of the previous state before the pre-transition state. The reasoning for this is that the component survived the stress in the state previous to the pre-transition state. B-6, observed by binary indicator; no break, therefore q(B-6) = 0. (Figure 3 shows the probability of failure of A-6).

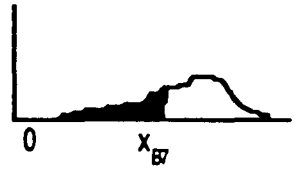

Figure 3. Probability of Failure of A-6.

The CDF parameters remain the same after transition because the strength of the components are not changed as a result of the break of a neighboring component (no shock wave, no shrapnel etc.) and the grv remains the same (same flight condition), but the stress (lrv) on the surviving components change with a change in configuration.

Continuing with the analysis of the algorithm:

C-6, observed by binary indicator; no break, therefore q(C-6) =0

A-4, already failed , excluded from set, no entry.

B-4, observed by binary indicator; a break, therefore calculate the probability of failure before the transition (B-6) and subtract the *survival* of the previous state before the pre-transition state(B-7). The failure of B occurred between 7 and 6, i.e. area under the pdf between $x_{B|7}$ (L) and $x_{B|6}$ (L). (Figure 4 graphically shows the value determined for the probability of failure of B-4).

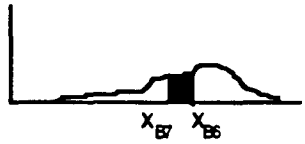

Figure 4. Probability of Failure of B-4.

C-4, observed by binary indicator; no break, therefore q(c-4) = 0

A-0; already failed; excluded from set, no entry

B-0; already failed; excluded from set, no entry

C-0, observed by binary indicator; a break, therefore calculate the probability of failure

before the transition (C-4) and subtract the survival of the previous state before the pre-transition state (C-6).

Summarizing the probability determination of the permutation 7640:

$$P(7\rightarrow 6\rightarrow 4\rightarrow 0 ; L \leq L) \equiv P(7640)$$
$$= \sum_{\text{all sequences}} P\{A \rightarrow \underline{A}\} \times P\{B \rightarrow \underline{B}\} \times P\{C \rightarrow \underline{C}\} \quad \text{by (12)}$$

In this case every box has either one transition with the associated probabilities or no transition with zero probability.

The probability of the sequence 7640 is the product of the transitional probabilities:

$$P(7640) = \{F_A[x_{A|7}(L)]\} \times \{F_B[x_{B|6}(L)] - F_B[x_{B|7}(L)]\} \times$$
$$\times \{F_C[x_{C|4}(L)] - F_C[x_{C|6}(L)]\}$$

If the strength of each component is independent of the transition, each component's CDF is the same before and after transition. Therefore, the probability reduces to:

$$P(7640) = \{F[x_{A|7}(L)]\} \times \{F[x_{B|6}(L)] - F[x_{B|7}(L)]\} \times \{F[x_{C|4}(L)] - F[x_{C|6}(L)]\}$$

If the components are identical, that is, e.g. same material and size, the CDF of each of the components are the same.

The probability of observing the 2nd bifurcation of the first branch of the failure tree is:

$$P(7\rightarrow 6\rightarrow 2\rightarrow 0 ; L \leq L) \equiv P(7620)$$

TABLE 6 formulates the probability for the second bifurcation of the first branch: 7620. The probability of observing the second bifurcation of the first branch of the failure tree is:

$$P(7620) = \{F_A[x_{A|7}(L)]\} \times \{F_B[x_{B|6}(L)] - F_B[x_{B|7}(L)]\} \times \{F_C[x_{C|4}(L)] -$$
$$- F_C[x_{C|6}(L)]\}$$

Table 7 formulates the probability of observing the 3rd bifurcation of the first branch of the failure tree. The probability of observing the 3rd bifurcation of the first branch of the failure tree is:

$$P(760) = \{F_A[x_{A|7}(L)]\} \times \{F_B[x_{B|6}(L)] - F_B[x_{B|7}(L)]\} \times \{F_C[x_{C|6}(L)] - F_C[x_{C|7}(L)]\}$$

TABLE 6. FORMULATION OF SECOND BIFURCATION FIRST BRANCH

State Indicator		Probability of Failure of Component $L \leq L$		
Binary	Octal	C	B	A
111	7			
110	6			$F_{A\|7}[x_{A\|7}(L)]$
010	2	$F_C[x_{C\|6}(L)]$- $F_C[x_{C\|7}(L)]$		
000	0		$F_B[x_{B\|2}(L)]$- $F_B[x_{B\|6}(L)]$	

TABLE 7. FORMULATION OF THIRD BIFURCATION FIRST BRANCH

State Indicator		Probability of Failure of Component $L \leq L$		
Binary	Octal	C	B	A
111	7			
110	6			$F_{A\|7}[x_{A\|7}(L)]$
000	0	$F_C[x_{C\|6}(L)]$- $F_C[x_{C\|7}(L)]$	$F_B[x_{B\|6}(L)]$- $F_B[x_{B\|7}(L)]$	

Table 8 formulates the probability of observing the last branch of the failure tree. The probability of observing the last bifurcation last branch of the failure tree is:

$$P(70) = \{F_A[x_{A|7}(L)]\} \times \{F_B[x_{B|7}(L)]\} \times \{F_C[x_{C|7}(L)]\}$$

4. The Algorithm

The algorithm to generate the probability of system failure given the component failure is as follows:

1. List all Octal representation (for completeness of combinations).
2. Observe by binary representation (for state indicator).
3. Calculate the probability of a failure of a sequence of consecutive states by:

Transition probability = state before transition - previous state before the pre-transition state.

Probability of entire sequence = product of the transitional probabilities.

The probability of failure of the system is the sum(union) of the probability of failure of each of the sequences by (12).

$$P\{system\} = P(7640)+P(7620)+P(760)+P(7540)+P(7510)+P(750)+P(7320)+P(7310) + \\ +P(730)+P(740)+P(720)+P(710)+P(70)$$

TABLE 8. FORMULATION OF PROBABILITY OF LAST BRANCH

State Indicator		Probability of Failure of Component $L \leq L$		
Binary	Octal	C	B	A
111	7			
000	0	$F_C[x_{C\|7}(L)]$	$F_B[x_{B\|7}(L)]$	$F_{A\|7}[x_{A\|7}(L)]$

5. Failure Combinations for Four Components

The failure combinations and their octal representation for components are presented in Table 9. The algorithm was applied to a system with four components. Appendix, TABLE 1, contains all the possible permutations (failure tree branches) for the system. Appendix, TABLE 2 provides the permutations for system failure given one component has failed. Appendix, TABLE 3 provides the permutations for system failure given two components have failed. Appendix, TABLE 4 provides the permutations for system failure given three components have failed.

Appendix, TABLE 5 provides the permutations for a failure of two components given one component has failed. Appendix, TABLE 6 provides the permutations for a failure of three components given one component has failed. Appendix, TABLE 7 provides the permutations for a failure three components given two components have failed.

The probability of the system for the above conditions can be determined by taking the product of each row in the table and then summing those products.

TABLE 9. OCTAL AND BINARY REPRESENTATION OF COMBINATION STATES

Octal Code	Binary States
Components--->	D C B A
15	1 1 1 1
14	1 1 1 0
13	1 1 0 1
12	1 1 0 0
11	1 0 1 1
10	1 0 1 0
9	1 0 0 1
8	1 0 0 0
7	0 1 1 1
6	0 1 1 0
5	0 1 0 1
4	0 1 0 0
3	0 0 1 1
2	0 0 1 0
1	0 0 0 1
0	0 0 0 0

III. FINITE ELEMENT STRESS ANALYSIS

The algorithm developed in the probability analysis requires an input of the random variable before the probability can be quantified. In the current application, the RV is stress in the spatial locations of all the failure sites. A finite element analysis of the tie bar leaf was conducted to determine the stress at the failure sites in all the possible damage configurations.

A. ANALYSIS METHOD OVERVIEW

Removal criteria for the tie bar is two broken straps on one tie bar leaf. Since the majority of failures have occurred on the top two and bottom two leaves, from field experience, analysis was conducted on the top two and the bottom two leaves. Since each leaf has four straps and each strap can only fail once, there are a total of 15 configurations of different failure states for each leaf. Each configuration was evaluated for 9 different load sets in the flight block. Each load set defined loads and displacements at 4 positions in one rotation of the rotor plane. Stress was recorded at four spatial locations on the tie bar, one on each component, for the four locations in the rotor plane. A schematic of the analysis hierarchy is presented in Figure 5.

A single leaf of the tie bar was modeled using version 1.70a of the COSMOS/M finite element program by Structural Research and Analysis Corporation of Santa Monica, California. The program was run on a PC compatible computer. The leaf was divided into 720, 4 node, linear quadrilateral thin shell elements . This element type provided bending and membrane capabilities for analysis of a three dimensional structural model. Six degrees of freedom per node were considered for structural analysis.

The damaged leaves were modeled by copying the undamaged model and removing elements from the damaged straps of the respective configuration. The elements removed were those corresponding to the spatial location of maximum Mises stress experienced by the undamaged tie bar leaf. The locations correlated with the field experience locations where failure usually occurs.

The tie bar leaf model is presented in Figure 6.

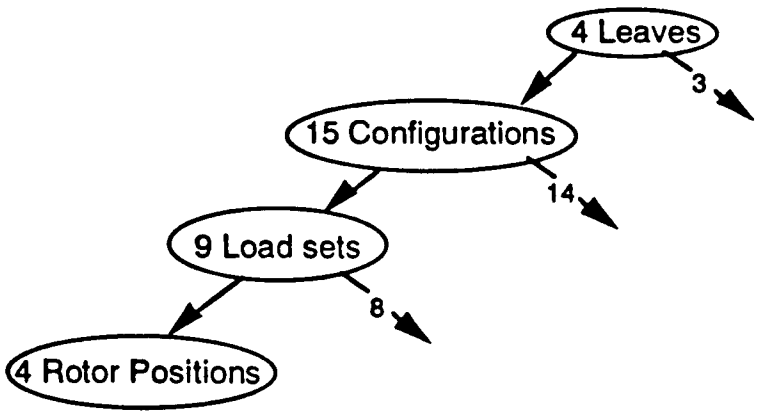

Figure 5. Analysis Hierarchy

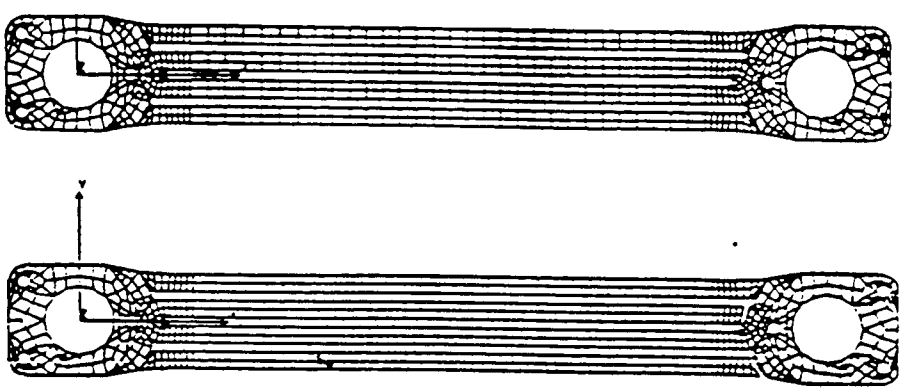

Figure 6. Finite Element Tie Bar Leaf, Undamaged (top), Damaged (bottom).

A leaf model was rendered for all possible combinatorial failure states of the leaf. Component failure was modeled by removal of elements at locations where the tie bar straps have historically failed. The flight load block provided by the Naval Aviation Depot, Cherry Point, North Carolina was used to establish the boundary conditions for the analysis. Kinematic analysis of the rotor system and the tie bar was used to properly apply the flight load block boundary conditions to the leaf. Solutions were obtained for boundary conditions of unit displacements in the longitudinal, lateral, torsional, and bending degrees of freedom. The analysis process was repeated for each of these models. The maximum and minimum Mises stress was obtained from the finite element program.

B. LEAF MODEL

The tie bar consists of 35 identical leaves of AISI 301 stainless steel stacked with 34 stainless shims in between them. The tie bar is constructed in such a way as to provide strength along the longitudinal and lateral axes while providing low torsional rigidity to allow rotation about the longitudinal axis and low bending rigidity to allow rotation about the transverse axis. The leaves are hydraulically pressed together and held together by bushings passing through pin holes at either end. If the pressed stack is less than a specified height, another leaf is pressed onto the stack. TABLE 10 contains the material constants of AISI 301 Stainless Steel.

TABLE 10. MATERIAL CONSTANTS OF AISI 301

Material Constant	Value
Modulus of Elasticity x-direction	2.6×10^7 psi
Modulus of Elasticity y-direction	2.8×10^7 psi
Poisson Ratio (x-y)	0.28

Only one leaf was modeled to represent all the leaves in the stack. The given nominal values for leaf and shim thickness were used for the analysis so that the simplifying

assumption could be made that all leaves were identical in size. Since all leaves were assumed identical the solution for a single leaf could be scaled to obtain a solution for any leaf in the stack. TABLE 11 lists the mean thickness values used in modeling the leaf. All dimensional values were obtained from manufacturing drawings provided by the contractor.

TABLE 11. NOMINAL PHYSICAL THICKNESS VALUES

Component	Notation	Thickness(in)
Tie Bar	T	1.43
Tie Bar Leaf	t	0.035
Tie Bar Shim	s	0.006

C. BOUNDARY CONDITIONS

The Appendix, TABLE 8 lists the flight regime and boundary conditions of the flight block. The given flight load block provided boundary conditions in both force and displacement values.

A kinematic analysis of the rotor system was conducted to establish the phasing of the loads and the kinematics of the tie bar.

1. Rotor System

Figure 7 shows the sign convention of the rotor system. The H-46 rotor system is a fully articulated system. A fully articulated rotor system is a system that provides hinges to allow for independent in plane (lead-lag) and out of plane (flapping) motion of each rotor blade.

Flapping of the blades occurs because the relative velocity on the blade advancing into the direction of the flight is greater than that on the blade retreating from forward flight. Thus, more lift is produced on the advancing blade than on the retreating blade. The flapping hinge allows the blade to flap upward and the retreating blade to flap downward

preventing a rolling moment on the helicopter. The climbing of the advancing blade and diving of the retreating blade decrease and increase the angle of attack respectively. The change in angle of attack changes the lift distribution on the blade. [Ref 5, p 142-145] Figure 8 shows the effect of rotor flapping on lift distribution.

The rotor attains equilibrium when the local changes in angle of attack are just sufficient to compensate for the local changes in dynamic pressure. Maximum upward flapping angle is attained at Ψ=180 where the local velocity is reduced to its mean forward flight value and the maximum downward flapping angle is attained at Ψ=0 where local velocity is also at a mean. The maximum flatwise bending moment which causes the blade to accelerate upward or downward occurs at Ψ=90→120 (upward) and Ψ=270 (downward) respectively. [Ref 6, p 107, 120]

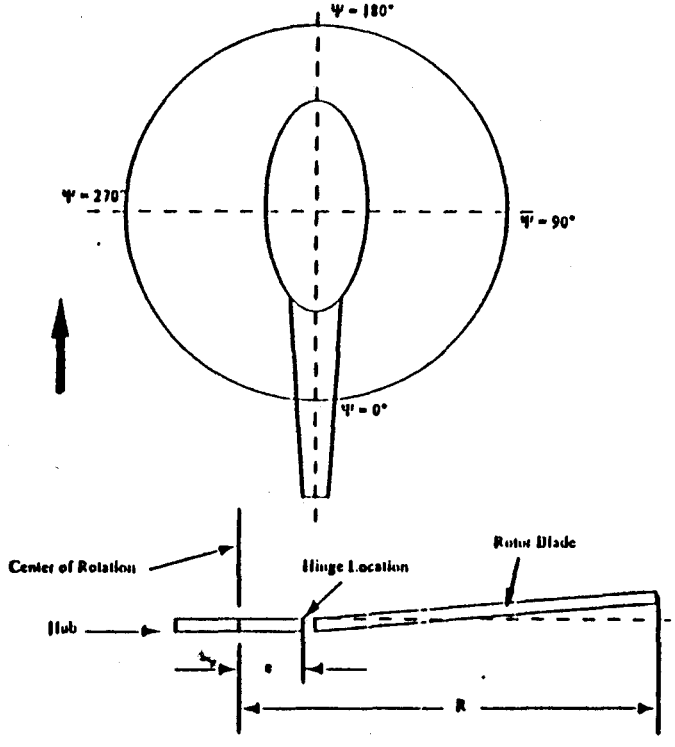

Figure 7 Rotor System Sign Convention.

Leading and lagging is caused by inplane moments produced by a combination of cyclically varying drag and inertia loads. The inertia loads are related to the flapping action

of the blade. The blades center of gravity moves toward the center of rotation (the hub) as it flaps up. Since the product of the moment of inertia of the blade and the rate of spin must remain constant, the blade tries to accelerate inplane to compensate for the change in its moment of inertia. This change in inertia of the rotor system is resisted by the inertia of the other blades so the blade tries to bend forward producing a moment. [Ref. 5:p. 147] A vertical lead-lag hinge allows the blade to accelerate forward.

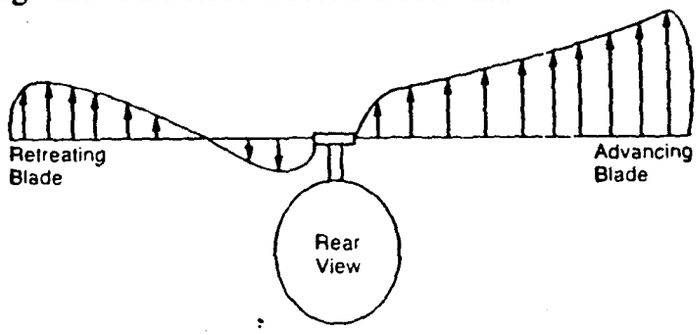

(a) Lift Distribution without Flapping

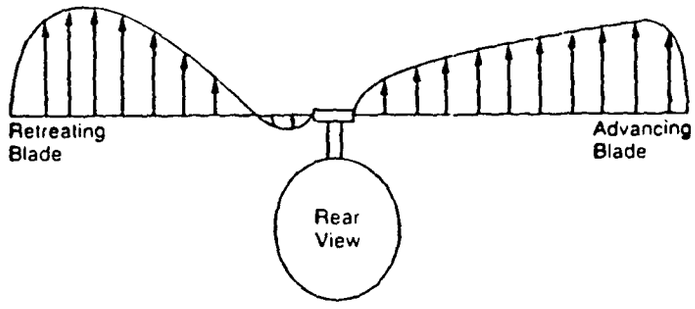

(b) Lift Distribution with Flapping

Figure 8. Effects of Blade Flapping on Lift Distribution.

2. Phasing of Loading, Twisting, and Bending

The phasing of the loads will determine how to apply the boundary conditions to the tie bar to most accurately model the boundary conditions in flight. Centrifugal force is always present and is relatively constant throughout one revolution of the blade, the oscillation caused by lead-lag is negligible when compared to the mean value. The twist or feathering of the blade is a displacement boundary condition dictated by the setting of the cyclic and collective controls. Minimum feathering is set at Ψ=90 and maximum is set at

Ψ=270 with the mean occurring at Ψ=0 and Ψ=180. The phasing of the minimum and maximum values of the rotor forces and moments as a function of Ψ are presented in TABLE 12.

TABLE 12. PHASING OF THE FLIGHT LOADS AND DISPLACEMENTS

Rotor Position (Ψ)	Centrifugal Force	Feathering	Bending
0	constant	mean	mean
90	constant	minimum	max up
180	constant	mean	mean
270	constant	maximum	max down

3. Specific Kinematics of Tie Bar Mechanism

The specific kinematics of the rotor system with respect to the tie bar were analyzed so that the boundary conditions could be applied correctly. Figure 9 shows the Tie Bar and Pitch Varying Assembly.

The tie bar is encased in two concentric aluminum tubes called the pitch varying assembly, each allowed to rotate about roller bearings and slide axially independent of the other. The tie bar assumes all the axial load caused by the centrifugal force on the blade due to rotation. The outer tube transmits the desired feathering deflection from the pitch change horn to the blade. A twisting displacement is applied to the tie bar due to this feathering displacement. The flatwise bending moment due to flapping applies a bending moment into the concentric tube assembly. The tubes take the majority of the bending load but the tie bar deflects as shown in Figure 9. The deflection of the tubes causes a bending deflection in the tie bar.

4. Resolution of the Boundary Conditions into Displacements

The kinematics of the tie bar under the described loads and displacements is presented in Figure 10. The boundary conditions in the flight load block were given as two displacements and a force.

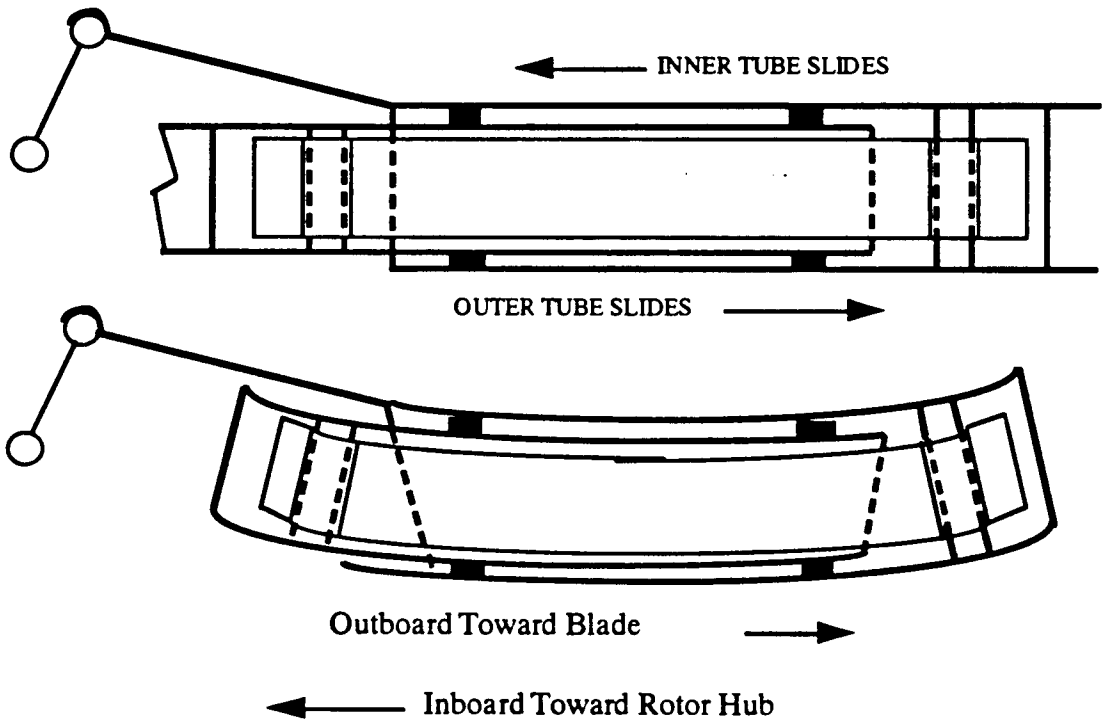

Figure 9. Tie Bar and Pitch Varying Assembly.

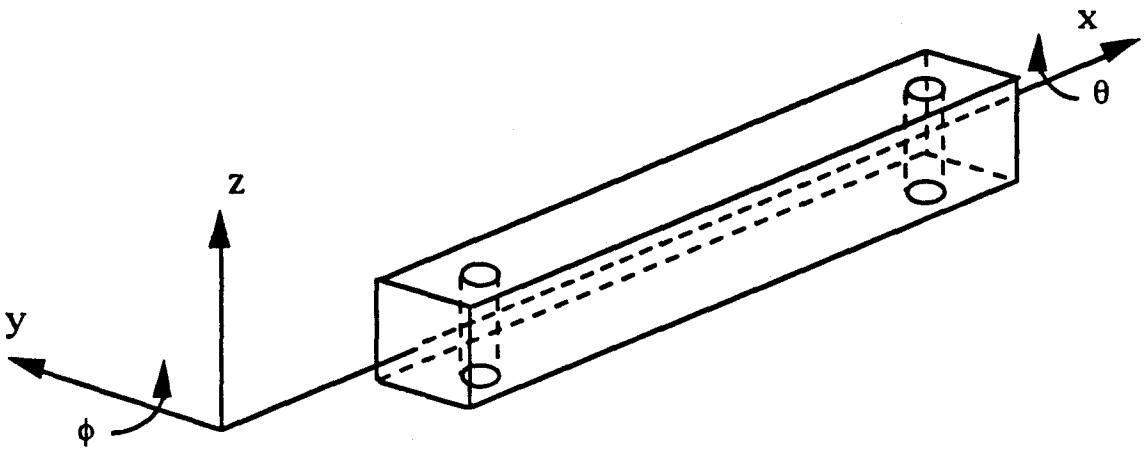

Force in X direction

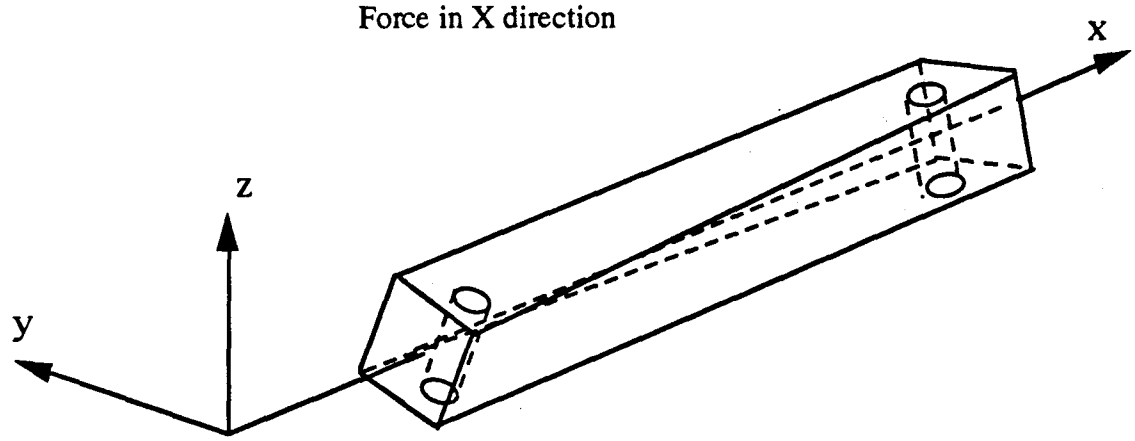

Twist about the X axis; θ

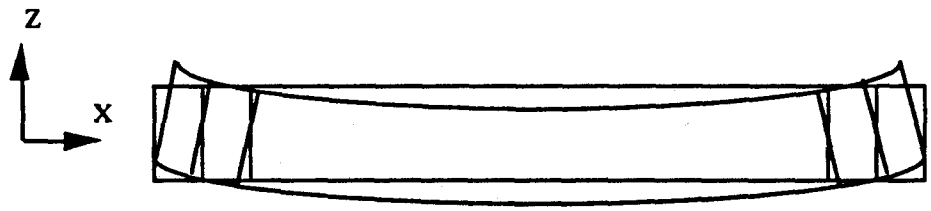

Bending About the Y axis; ϕ

Figure 10. Tie Bar Kinematics.

The kinematic analysis of the tie bar allowed the boundary conditions to be transformed into four displacements. Figure 11 is a rendering of the tie bar pin hole as it is rotated through an angle of θ or ϕ.

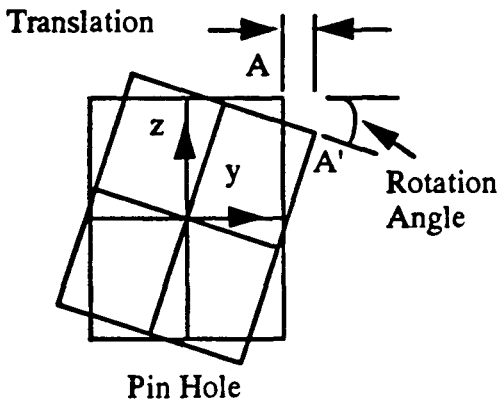

Figure 11. Tie Bar Pin Hole.

Rotation of the pin hole causes displacement of A from A to A'. The displacement can be decomposed into a rotation about the neutral axis and a translation parallel to the transverse axis. The value of the translation is dependent on the distance of the point from the neutral axis. A rotation for a leaf at the neutral axis would be resolved into a rotation only. Thus, rotation about the X axis, θ, can be resolved into a rotation about the x axis and a translation parallel to the y axis. A Bending about the y axis, ϕ, can be resolved into a rotation about the y axis and a translation parallel to the x axis.

Boundary conditions were applied at the nodes on the tie bar leaf pin holes. A feature of the program allowed the definition of the pin hole as a contour. The boundary conditions could be applied to the two pin hole contours.

Solutions were obtained for four separate cases to verify that applying the boundary conditions using the contour feature provided the same results as applying the boundary conditions at the nodes on the pin hole independently. A unit displacement in the x direction was applied to the contours and then the independent nodes. The stresses, strains, and displacement provided in the solution files were compared and were identical.

A similar procedure was repeated for displacement in the y direction. Unit rotations about both the x and y axes were also checked. An angular displacement was applied at the contours. Nodal inputs were determined by resolving the rotation of the pin hole at the neutral axis into two translations. A rotation about the x axis was resolved into translations in the y and z axes. A rotation about the y axis was resolved into a translation in the x and z axes. The solutions matched.

Initial solutions were obtained for each configuration by applying a translation in x, a translation in y, a rotation about x, and a rotation about y of 0.1 in opposite directions at the pin holes contours. Another feature of the program combined and scaled the inputs to obtain solutions for different load conditions. The feature was verified by running a combined load case and comparing the solutions to a case using the combination feature.

5. Calculating the Scaling Factors

Solutions were obtained for deflections shown in Appendix A, TABLE 8, by scaling the results obtained for the 0.1 unit deflections. Scaling for the undamaged leaf was accomplished using the following equations:

Rx scaling factor = Rx desired/0.2

Uy scaling factor = ((Z)*sin(Rx desired))/0.2

Ry scaling factor = Ry desired/0.2

where:

Z = the vertical distance from the center of the tie bar.

The centrifugal force boundary condition was resolved for two different cases. First, the condition was resolved for the case where the leaf is undamaged. The force, f, resulting from the 0.1 unit deflection on each pin hole was obtained from the program. The value was multiplied by 35 to obtain the resultant force, F, on the entire tie bar. The scaling factor was calculated by dividing the desired force by the resulting force.

Ux scaling factor = Fx desired/F

The translation in x resolved from the bending rotation about y must also be subtracted from the force scaling factor.

Ux scaling factor = Fx desired/F+((Z)*sin(Ry desired))/0.2

When modeling a damaged leaf's boundary conditions, compatibility and equilibrium between the damaged leaf and the 34 undamaged leaves had to be satisfied. The force on a damaged leaf was calculated for a 0.1 unit deflection using the finite element program. The resultant force on the damaged leaf, f', was added to 34 times f to obtain the total resultant force on the damaged tie bar, F', corresponding to the applied 0.1 unit deflection. The scaling factor applied to the 0.1 unit displacement of the damaged leaf to obtain the desired resultant force, F_X desired, is:

Ux scaling factor= F_X desired/F'

Combining this scaling factor with the translation in x resolved from the bending rotation about the y axis:

Ux scaling factor = F_X desired/F' + ((Z)*sin(Ry desired))/0.2

6. Applying Symmetry

Symmetry of the leaf about its neutral axis was used to reduce the number of combinatorial states. The leaf was symmetric about the x axis. Some combinatorial states were physically equivalent with others. Only one member of each equivalent pair needed to be analyzed to obtain the solution for both members. Equivalent states are presented in TABLE 13. The application of symmetry reduced the number of combinatorial states that required analysis from fifteen to ten.

TABLE 13. SYMMETRIC GEOMETRIC STATES

States		Equivalence	
Octal	Binary	Octal	Binary
14	1110	7	0111
13	1101	11	1011
12	1100	3	0011
10	1010	5	0101
8	1000	1	0001
4	0100	2	0010

D. MISES STRESS

The boundary conditions as described generate a combined state of stress. Depending on the failure mechanisms, different failure criteria are used to reduce the combined stress tensor to a single scalar equivalent stress. Maximum principal stress is used for brittle material where crack propagation occurs perpendicular to the maximum principal stress. Maximum shear stress (Tresca Criteria) is used for ductile material. [Ref. 2:p. 244]

Experimental evidence on steel in combined states of stress tend to favor the failure criterion proposed by Von Mises. The equivalent stress term, the Mises stress is defined as:

$$\sigma_e = \frac{1}{\sqrt{2}}\left[(\sigma_1 - \sigma_2)^2 + (\sigma_2 - \sigma_3)^2 + (\sigma_3 - \sigma_1)^2\right]^{1/2}$$

where,

$\sigma_{1,2,3}$ = the principal stresses

The calculation of the Mises stress is implemented in the COSMOS/M software.

E. DATA REDUCTION

The maximum and minimum Mises stress was determined in the following manner. The program queried each element for the maximum Mises stress. The Mises stress could be tabulated from highest to lowest. A map of the leaf's numbered finite elements was used to determine the spatial location of the maximum Mises stress on the four straps of the leaf. The maximum Mises stress was sought on each of the four straps for each of the four values of Ψ, which represented one load cycle. The maximum Mises stress on a strap for one cycle was recorded along with the element location at which it occurred. Once the maximum Mises stresses for the cycle were recorded, the minimum stress for the cycle at the same location was sought. The two values for each strap were used as the maximum and minimum cyclic stress for the load set. The procedure was used for each combinatorial stress state.

V. FATIGUE ANALYSIS

Engineering fatigue analysis using the methodology outlined in chapter II can, at best, predict the mean life under constant amplitude load histories. For applications where the load history is not constant, cumulative damage modifications such as Miner's rule are used. The variability of fatigue life is sometimes addressed by specifying the design life to be a multiple of service life. In view of the unexpected failures in the field experience of the H-46 tie bars, explicit treatment of the life distribution is prudent.

Fatigue damage is dependent on the applied stress level and duration of load application, the general form of cumulative distribution of fatigue must be a joint distribution of stress (σ) and time (t):

$F(\sigma,t)$

A general probabilistic functional form was originally proposed by Coleman (1958) and recast into engineering analysis by Phoenix and Wu [Ref. 7, p. 140]. The application of this formulation is described in the following.

A. CUMULATIVE DAMAGE INCLUDING PROBABILISTIC EFFECTS

Based on the materials sciences understanding of the failure process of stainless steel, dimensions of the flaw are chosen to be the parameters for characterizing the strength and life of the tie bar. The flaws are considered to be a random occurrence intrinsic to the material and the fabrication process of the tie bar leaf. The occurrence of the flaw is measured by an arbitrary metric volume within which the random variable, stress, is uniform. The range of these intrinsic flaws are:

$0 < a < a_c$

where the critical flaw size, a_c, is related to the fracture toughness of the specific material:

$$k_c = \sigma\sqrt{a_c}$$

The probability of occurrence of flaws greater than a in metric volumes within each structural component (the leaf of the tie bar) is binomially distributed.

$$f(n) = C_n\, p^n\, (1-p)^{(N-n)};$$

where

$p = P(a > a_C)$;

N = number of metric volumes

n = number of flaws $a > a_C$

For the tie bar to have a life greater than zero, the average flaw size must be much less than a_C. For a material of serviceable uniformity, the probability of occurrence of a flaw greater than size a within any metric volume must be very small. In order for the stress to be uniform the number of metric volumes must be large. If the flaw density is low, $p<<1$, and the number of metric volumes is large, $N>>1$, then:

$$\ln(1-p) \approx -p$$

and

$$f(n) = (\mu^n / n!)e^{-\mu}$$

where μ is a parameter. Thus, the hazard, $\Psi(\tau)$, is poissonly distributed:

$$F(t|\sigma) = 1-\exp[-\Psi(\tau)]$$

where

t = the random variable time

$\tau = t/t_o$; t_o is some intrinsic (normalizing) time constant

When the failure is homogeneous to the system, that is, the failure process for the system is the same as for the metric volume, the hazard, $\Psi(\tau)$, takes on the Weibull form:

$$\Psi(\tau) = \tau^{\alpha}$$

The hazard must be increasing; the damage is never repaired, and unbounded; the system has a finite life.

B. DAMAGE ACCUMULATION

The intrinsic (normalized) time is convoluted in the break down rule k:

$$\tau = \frac{1}{t}\int_{o}^{t_f} \kappa[\sigma(t)]dt$$

where:

τ = the fractional life

t = intrinsic time constant

The time is normalized to obtain fractional life. Fractional life non-dimensionally indicates life used. Thus, the probability of failure of one of the components given the stress on the component, σ, and the time at which the probability is desired, t, the breakdown rule, κ, and its parameters is:

$$F(t|\sigma) = 1 - \exp\left[-\left\{\frac{1}{t}\int_{0}^{t_f} \kappa\left[\sigma(t)dt\right]\right\}^{\alpha}\right]$$

C. BREAKDOWN RULE

Different physical breakdown processes give rise to different forms of $\kappa\{\sigma(t)\}$. The power form is:

$$\kappa[\sigma(t)] = \left[\frac{\sigma(t)}{\sigma_o}\right]^{\rho}$$

When using the power form, the life is bounded for low stress levels. It is observed to fit low cycle fatigue data where the system is subjected to high stress and low cycles to failure. The form is used for ductile metals associated with yielding. The power form plots as a straight line on the log-log axes, as shown in Figure 11.

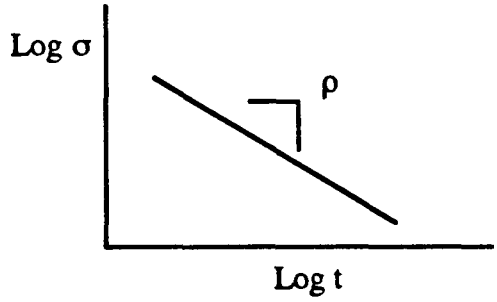

Figure 11. Plot of Power Form Breakdown Rule.

The exponential form is:

$$\kappa[\sigma(t)] = \sigma_i \exp\left[\frac{\sigma(t)}{\sigma_o}\right]$$

When using the exponential form the life of the system is unbounded for low stress levels. It is observed to fit high cycle fatigue data where the stress is low and the system is subjected to a high number of cycles to failure. The exponential form plots as a straight line on semi-log axes, as shown in Figure 12.

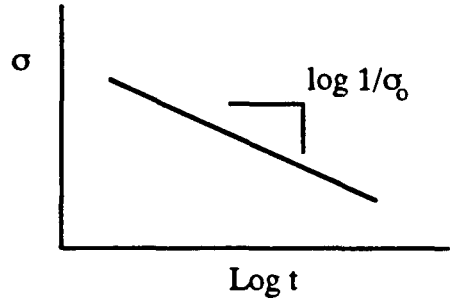

Figure 12. Plot of Exponential Form Breakdown Rule.

D. METHODOLOGY

Data is collected for one history for which the stress ratio, R, and the applied load amplitude are held constant until failure. Stress analysis is conducted on the specimen for the applied load so that the load can be mapped into the random variable of stress. The stress-life data are plotted as shown is Figure 13.

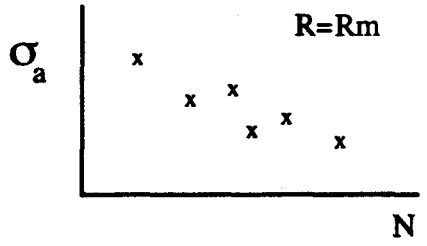

Figure 13. Plot of Load History Data.

The data is analyzed for trends. The domain of interest is chosen. The domain of interest is the life region for which predictions are required. A model of the breakdown rule is chosen based on the failure mode(yield, fracture) and the model is calibrated to the data to obtain the model's parameters as shown in Figure 14.

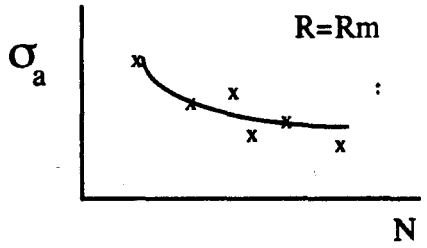

Figure 14. Model Calibrated to the Data.

E. VERIFICATION

Data is obtained for a second history for which R is different than the previous R, say R1. A number of specimens are tested, each at a different constant stress amplitude, σ_a. The model is transformed into the new data or D1 domain, as shown in Figure 15. The D1 data is plotted and the model is assessed for goodness of prediction. The verification process is repeated a second time at a different R, R2, resulting in data D2, as shown in Figure 16. The second verification increases our confidence in the model.

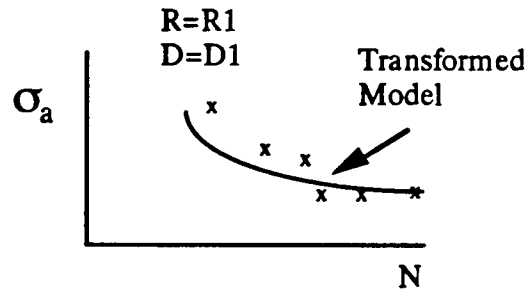

Figure 15. Model Transformed Into D1 Domain.

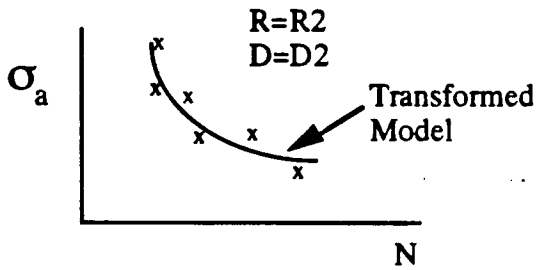

Figure 16. Model Transformed Into D2 Domain.

Data are now collected to gain a perspective of the damage cumulation integral. Specimens are subjected to a history sequence of σ_{a1} with a stress ratio R1 for n_1 cycles and then subjected to σ_{a2} with a stress ratio R2 for n_2 cycles. The data, D12, are collected. The model is transformed into the D12 domain using the cumulation integral. The breakdown rule is integrated for σ_{a1} from time t_1 to t_2 and for σ_{a2} from t_2 to t_3. This verification will confirm that either Miner's Rule may be used or that non-linear superposition is required.

VI. RESULTS

The finite element analysis and fatigue analysis have resulted in the probability of failure of a component of the tie bar leaf given the configuration, the flight load block and the time the component is exposed to the loads; the flight time. The probability of the component for a given configuration (state) can be collapsed to one value on a spread sheet. The algorithms developed and presented in Appendix A have been developed on an EXCEL spread sheet. The total probability of the system failing given an initial state of one, two ,or three failed components can be calculated once the stress life model is calibrated and the convolution form is determined. The probability of a system transitioning to a final state of one, two, or three failed, given an initial state of one, two, or three failed can also be calculated.

VII. CONCLUSIONS

The primary objective of this research was to develop a method of determining the reliability of the H-46 helicopter tie bar given the amount of flight time experienced by the tie bar. The stress life must be calibrated for using the supplied field data. Once the model has been calibrated, the model can be used by the Navy and Marine Corp in three different ways.

First, the method can be used to determine whether the reliability of the tie bar is sufficient to fly an aircraft past a certain amount of flight time. Second, the method can determine provisioning requirements for the tie bar given the amount of flight time expected over a certain time period. Finally, the failure rate of the tie bar can be calculated and thus the required inspection cycle set to preclude inadvertent failure. This information can be used to set a NATOPS limit for continuous flight time without inspection.

VII. RECOMMENDATIONS

A stress life model of the tie bar needs to be calibrated for the given field data. The model can then be used as stated in Chapter VI.

The algorithm needs to be generalized to the extent that the probability can be calculated using a computer program. The user would input the initial and final state, the number of components and the stress on each component in each configuration. The output would be the probability of failure of the system in the given initial state.

The probability analysis should be applied to multiple leaves of the tie bar so that the probability of failure of more than one leaf can be calculated. The failure of components in one leaf would change the boundary conditions on the other leaves. More stress analysis would be required to determine the stress on other leaves given the failure of components on one or more other leaves.

A new flight block has been provided by the contractor and will be used to bench test the new tie bars in a test jig. The stresses corresponding to the new flight block should be generated using the finite analysis model and the model then used to validate the data.

The method should be used to test the new designs proposed to solve the failure problem. The method could be applied to the new tie bar that has minor geometric changes, by modifying the geometry of the finite element model.

LIST OF REFERENCES

1. Allen, D. H., Haisler, W. E., *Introduction to Aerospace Structural Analysis,* John Wiley & Sons, Inc., p. 399, 1985.

2. Bannintine, J. A., Comer, J. J., and Handrock, J. L., *Fundamentals of Metal Fatigue Analysis,* Prentice-Hall, Inc., p. 232-235, 1990.

3. Lewis, E. E., *Introduction to Reliability Engineering,* John Wiley & Sons, Inc., p. 10-16, 1986.

4. DeGroot, M. H., *Probability and Statistics,* Addison-Wesley, p. 55-56,1975.

5. Prouty, R. W., *Helicopter Performance, Stability, and Control,* Prindle, Weber, & Schmidt, p. 142-145, 1986.

6. U.S. Army Transportation Research Command technical report 64-15, , *Parametric Investigation of the Aerodynamic and Aeroelastic Characteristics of Articulated and Rigid (hingeless) Helicopter Rotor Systems,* by Sikorsky Aircraft Company, p. 107, 120, 1964.

7. Phoenix, S. L. and Wu, E. M., "Statistics for the Time Dependent Failure of Kevlar-49/Epoxy Composites: Micromechanical Modeling and Data Interpretation," paper presented at the IUTAM Symposium on Mechanics of Composite Materials, Virginia Polytechnic Institute and State University, Blacksburg, Virginia, 16-19 August 1982.

APPENDIX

TABLE 1. PROBABILITY OF TOTAL SYSTEM FAILURE

Failure Sequences	Probability of Failure of Component L ≤ L			
	D	C	B	A
15 14 12 8 0	$F_D[x_{D\|8}(L)] - F_D[x_{D\|12}(L)]$	$F_C[x_{C\|12}(L)] - F_C[x_{C\|14}(L)]$	$F_B[x_{B\|14}(L)] - F_B[x_{B\|15}(L)]$	$F_A[x_{A\|15}(L)] - 0$
15 14 12 4 0	$F_D[x_{D\|12}(L)] - F_D[x_{D\|14}(L)]$	$F_C[x_{C\|4}(L)] - F_C[x_{C\|12}(L)]$	$F_B[x_{B\|14}(L)] - F_B[x_{B\|15}(L)]$	$F_A[x_{A\|15}(L)] - 0$
15 14 12 0	$F_D[x_{D\|12}(L)] - F_D[x_{D\|14}(L)]$	$F_C[x_{C\|12}(L)] - F_C[x_{C\|14}(L)]$	$F_B[x_{B\|14}(L)] - F_B[x_{B\|15}(L)]$	$F_A[x_{A\|15}(L)] - 0$
15 14 10 8 0	$F_D[x_{D\|8}(L)] - F_D[x_{D\|10}(L)]$	$F_C[x_{C\|14}(L)] - F_C[x_{C\|15}(L)]$	$F_B[x_{B\|10}(L)] - F_B[x_{B\|14}(L)]$	$F_A[x_{A\|15}(L)] - 0$
15 14 10 2 0	$F_D[x_{D\|10}(L)] - F_D[x_{D\|14}(L)]$	$F_C[x_{C\|14}(L)] - F_C[x_{C\|15}(L)]$	$F_B[x_{B\|2}(L)] - F_B[x_{B\|10}(L)]$	$F_A[x_{A\|15}(L)] - 0$
15 14 10 0	$F_D[x_{D\|10}(L)] - F_D[x_{D\|14}(L)]$	$F_C[x_{C\|14}(L)] - F_C[x_{C\|15}(L)]$	$F_B[x_{B\|10}(L)] - F_B[x_{B\|14}(L)]$	$F_A[x_{A\|15}(L)] - 0$
15 14 8 0	$F_D[x_{D\|8}(L)] - F_D[x_{D\|14}(L)]$	$F_C[x_{C\|14}(L)] - F_C[x_{C\|15}(L)]$	$F_B[x_{B\|14}(L)] - F_B[x_{B\|15}(L)]$	$F_A[x_{A\|15}(L)] - 0$
15 14 6 4 0	$F_D[x_{D\|14}(L)] - F_D[x_{D\|15}(L)]$	$F_C[x_{C\|4}(L)] - F_C[x_{C\|6}(L)]$	$F_B[x_{B\|6}(L)] - F_B[x_{B\|14}(L)]$	$F_A[x_{A\|15}(L)] - 0$
15 14 6 2 0	$F_D[x_{D\|14}(L)] - F_D[x_{D\|15}(L)]$	$F_C[x_{C\|6}(L)] - F_C[x_{C\|14}(L)]$	$F_B[x_{B\|2}(L)] - F_B[x_{B\|6}(L)]$	$F_A[x_{A\|15}(L)] - 0$
15 14 6 0	$F_D[x_{D\|14}(L)] - F_D[x_{D\|15}(L)]$	$F_C[x_{C\|6}(L)] - F_C[x_{C\|14}(L)]$	$F_B[x_{B\|6}(L)] - F_B[x_{B\|14}(L)]$	$F_A[x_{A\|15}(L)] - 0$
15 14 4 0	$F_D[x_{D\|14}(L)] - F_D[x_{D\|15}(L)]$	$F_C[x_{C\|4}(L)] - F_C[x_{C\|14}(L)]$	$F_B[x_{B\|14}(L)] - F_B[x_{B\|15}(L)]$	$F_A[x_{A\|15}(L)] - 0$
15 14 2 0	$F_D[x_{D\|14}(L)] - F_D[x_{D\|15}(L)]$	$F_C[x_{C\|14}(L)] - F_C[x_{C\|15}(L)]$	$F_B[x_{B\|2}(L)] - F_B[x_{B\|14}(L)]$	$F_A[x_{A\|15}(L)] - 0$
15 14 0	$F_D[x_{D\|14}(L)] - F_D[x_{D\|15}(L)]$	$F_C[x_{C\|14}(L)] - F_C[x_{C\|15}(L)]$	$F_B[x_{B\|14}(L)] - F_B[x_{B\|15}(L)]$	$F_A[x_{A\|15}(L)] - 0$
15 13 12 8 0	$F_D[x_{D\|8}(L)] - F_D[x_{D\|12}(L)$	$F_C[x_{C\|13}(L)] - F_C[x_{C\|12}(L)]$	$F_B[x_{B\|15}(L)] - 0$	$F_A[x_{A\|13}(L)] - F_A[x_{A\|15}(L)]$
15 13 12 4 0	$F_D[x_{D\|13}(L)] - F_D[x_{D\|12}(L)]$	$F_C[x_{C\|4}(L)] - F_C[x_{C\|12}(L)]$	$F_B[x_{B\|15}(L)] - 0$	$F_A[x_{A\|13}(L)] - F_A[x_{A\|15}(L)]$
15 13 12 0	$F_D[x_{D\|13}(L)] - F_D[x_{D\|12}(L)]$	$F_C[x_{C\|13}(L)] - F_C[x_{C\|12}(L)]$	$F_B[x_{B\|15}(L)] - 0$	$F_A[x_{A\|13}(L)] - F_A[x_{A\|15}(L)]$
15 13 9 8 0	$F_D[x_{D\|8}(L)] - F_D[x_{D\|9}(L)]$	$F_C[x_{C\|13}(L)] - F_C[x_{C\|15}(L)]$	$F_B[x_{B\|15}(L)] - 0$	$F_A[x_{A\|9}(L)] - F_A[x_{A\|13}(L)]$
15 13 9 1 0	$F_D[x_{D\|9}(L)] - F_D[x_{D\|13}(L)]$	$F_C[x_{C\|13}(L)] - F_C[x_{C\|15}(L)]$	$F_B[x_{B\|15}(L)] - 0$	$F_A[x_{A\|1}(L)] - F_A[x_{A\|9}(L)]$
15 13 9 0	$F_D[x_{D\|9}(L)] - F_D[x_{D\|13}(L)]$	$F_C[x_{C\|13}(L)] - F_C[x_{C\|15}(L)]$	$F_B[x_{B\|15}(L)] - 0$	$F_A[x_{A\|9}(L)] - F_A[x_{A\|13}(L)]$
15 13 8 0	$F_D[x_{D\|8}(L)] - F_D[x_{D\|13}(L)]$	$F_C[x_{C\|13}(L)] - F_C[x_{C\|15}(L)]$	$F_B[x_{B\|15}(L)] - 0$	$F_A[x_{A\|13}(L)] - F_A[x_{A\|15}(L)]$
15 13 5 4 0	$F_D[x_{D\|13}(L)] - F_D[x_{D\|15}(L)]$	$F_C[x_{C\|4}(L)] - F_C[x_{C\|5}(L)]$	$F_B[x_{B\|15}(L)] - 0$	$F_A[x_{A\|5}(L)] - F_A[x_{A\|13}(L)]$
15 13 5 1 0	$F_D[x_{D\|13}(L)] - F_D[x_{D\|15}(L)]$	$F_C[x_{C\|5}(L)] - F_C[x_{C\|13}(L)]$	$F_B[x_{B\|15}(L)] - 0$	$F_A[x_{A\|1}(L)] - F_A[x_{A\|5}(L)]$
15 13 5 0	$F_D[x_{D\|13}(L)] - F_D[x_{D\|15}(L)]$	$F_C[x_{C\|5}(L)] - F_C[x_{C\|13}(L)]$	$F_B[x_{B\|15}(L)] - 0$	$F_A[x_{A\|5}(L)] - F_A[x_{A\|13}(L)]$

15	13	4	0		$F_D[x_{D\|13}(L)] - F_D[x_{D\|15}(L)]$	$F_C[x_{C\|4}(L)] - F_C[x_{C\|13}(L)]$	$F_B[x_{B\|15}(L)] - 0$	$F_A[x_{A\|13}(L)] - F_A[x_{A\|15}(L)]$
15	13	1	0		$F_D[x_{D\|13}(L)] - F_D[x_{D\|15}(L)]$	$F_C[x_{C\|13}(L)] - F_C[x_{C\|15}(L)]$	$F_B[x_{B\|15}(L)] - 0$	$F_A[x_{A\|1}(L)] - F_A[x_{A\|13}(L)]$
15	13	0			$F_D[x_{D\|13}(L)] - F_D[x_{D\|15}(L)]$	$F_C[x_{C\|13}(L)] - F_C[x_{C\|15}(L)]$	$F_B[x_{B\|15}(L)] - 0$	$F_A[x_{A\|13}(L)] - F_A[x_{A\|15}(L)]$
15	12	8	0		$F_D[x_{D\|8}(L)] - F_D[x_{D\|12}(L)]$	$F_C[x_{C\|12}(L)] - F_C[x_{C\|15}(L)]$	$F_B[x_{B\|15}(L)] - 0$	$F_A[x_{A\|15}(L)] - 0$
15	12	4	0		$F_D[x_{D\|12}(L)] - F_D[x_{D\|15}(L)]$	$F_C[x_{C\|4}(L)] - F_C[x_{C\|12}(L)]$	$F_B[x_{B\|15}(L)] - 0$	$F_A[x_{A\|15}(L)] - 0$
15	12	0			$F_D[x_{D\|12}(L)] - F_D[x_{D\|15}(L)]$	$F_C[x_{C\|12}(L)] - F_C[x_{C\|15}(L)]$	$F_B[x_{B\|15}(L)] - 0$	$F_A[x_{A\|15}(L)] - 0$
15	11	10	8	0	$F_D[x_{D\|8}(L)] - F_D[x_{D\|10}(L)]$	$F_C[x_{C\|15}(L)] - 0$	$F_B[x_{B\|10}(L)] - F_B[x_{B\|11}(L)]$	$F_A[x_{A\|11}(L)] - F_A[x_{A\|15}(L)]$
15	11	10	2	0	$F_D[x_{D\|10}(L)] - F_D[x_{D\|11}(L)]$	$F_C[x_{C\|15}(L)] - 0$	$F_B[x_{B\|2}(L)] - F_B[x_{B\|10}(L)]$	$F_A[x_{A\|11}(L)] - F_A[x_{A\|15}(L)]$
15	11	10	0		$F_D[x_{D\|10}(L)] - F_D[x_{D\|11}(L)]$	$F_C[x_{C\|15}(L)] - 0$	$F_B[x_{B\|10}(L)] - F_B[x_{B\|11}(L)]$	$F_A[x_{A\|11}(L)] - F_A[x_{A\|15}(L)]$
15	11	9	8	0	$F_D[x_{D\|8}(L)] - F_D[x_{D\|9}(L)]$	$F_C[x_{C\|15}(L)] - 0$	$F_B[x_{B\|11}(L)] - F_B[x_{B\|15}(L)]$	$F_A[x_{A\|9}(L)] - F_A[x_{A\|11}(L)]$
15	11	9	1	0	$F_D[x_{D\|9}(L)] - F_D[x_{D\|11}(L)]$	$F_C[x_{C\|15}(L)] - 0$	$F_B[x_{B\|11}(L)] - F_B[x_{B\|15}(L)]$	$F_A[x_{A\|1}(L)] - F_A[x_{A\|9}(L)]$
15	11	9	0		$F_D[x_{D\|9}(L)] - F_D[x_{D\|11}(L)]$	$F_C[x_{C\|15}(L)] - 0$	$F_B[x_{B\|11}(L)] - F_B[x_{B\|15}(L)]$	$F_A[x_{A\|9}(L)] - F_A[x_{A\|11}(L)]$
15	11	8	0		$F_D[x_{D\|8}(L)] - F_D[x_{D\|11}(L)]$	$F_C[x_{C\|15}(L)] - 0$	$F_B[x_{B\|11}(L)] - F_B[x_{B\|15}(L)]$	$F_A[x_{A\|11}(L)] - F_A[x_{A\|15}(L)]$
15	11	3	2	0	$F_D[x_{D\|11}(L)] - F_D[x_{D\|15}(L)]$	$F_C[x_{C\|15}(L)] - 0$	$F_B[x_{B\|2}(L)] - F_B[x_{B\|3}(L)]$	$F_A[x_{A\|3}(L)] - F_A[x_{A\|11}(L)]$
15	11	3	1	0	$F_D[x_{D\|11}(L)] - F_D[x_{D\|15}(L)]$	$F_C[x_{C\|15}(L)] - 0$	$F_B[x_{B\|3}(L)] - F_B[x_{B\|11}(L)]$	$F_A[x_{A\|1}(L)] - F_A[x_{A\|3}(L)]$
15	11	3	0		$F_D[x_{D\|11}(L)] - F_D[x_{D\|15}(L)]$	$F_C[x_{C\|15}(L)] - 0$	$F_B[x_{B\|3}(L)] - F_B[x_{B\|11}(L)]$	$F_A[x_{A\|3}(L)] - F_A[x_{A\|11}(L)]$
15	11	2	0		$F_D[x_{D\|11}(L)] - F_D[x_{D\|15}(L)]$	$F_C[x_{C\|15}(L)] - 0$	$F_B[x_{B\|2}(L)] - F_B[x_{B\|11}(L)]$	$F_A[x_{A\|11}(L)] - F_A[x_{A\|15}(L)]$
15	11	1	0		$F_D[x_{D\|11}(L)] - F_D[x_{D\|15}(L)]$	$F_C[x_{C\|15}(L)] - 0$	$F_B[x_{B\|11}(L)] - F_B[x_{B\|15}(L)]$	$F_A[x_{A\|1}(L)] - F_A[x_{A\|11}(L)]$
15	11	0			$F_D[x_{D\|11}(L)] - F_D[x_{D\|15}(L)]$	$F_C[x_{C\|15}(L)] - 0$	$F_B[x_{B\|11}(L)] - F_B[x_{B\|15}(L)]$	$F_A[x_{A\|11}(L)] - F_A[x_{A\|15}(L)]$
15	10	8	0		$F_D[x_{D\|8}(L)] - F_D[x_{D\|10}(L)]$	$F_C[x_{C\|15}(L)] - 0$	$F_B[x_{B\|10}(L)] - F_B[x_{B\|15}(L)]$	$F_A[x_{A\|15}(L)] - 0$
15	10	2	0		$F_D[x_{D\|10}(L)] - F_D[x_{D\|15}(L)]$	$F_C[x_{C\|15}(L)] - 0$	$F_B[x_{B\|2}(L)] - F_B[x_{B\|10}(L)]$	$F_A[x_{A\|15}(L)] - 0$
15	10	0			$F_D[x_{D\|10}(L)] - F_D[x_{D\|15}(L)]$	$F_C[x_{C\|15}(L)] - 0$	$F_B[x_{B\|10}(L)] - F_B[x_{B\|15}(L)]$	$F_A[x_{A\|15}(L)] - 0$
15	9	8	0		$F_D[x_{D\|8}(L)] - F_D[x_{D\|9}(L)]$	$F_C[x_{C\|15}(L)] - 0$	$F_B[x_{B\|15}(L)] - 0$	$F_A[x_{A\|9}(L)] - F_A[x_{A\|15}(L)]$
15	9	1	0		$F_D[x_{D\|9}(L)] - F_D[x_{D\|15}(L)]$	$F_C[x_{C\|15}(L)] - 0$	$F_B[x_{B\|15}(L)] - 0$	$F_A[x_{A\|1}(L)] - F_A[x_{A\|9}(L)]$
15	9	0			$F_D[x_{D\|9}(L)] - F_D[x_{D\|15}(L)]$	$F_C[x_{C\|15}(L)] - 0$	$F_B[x_{B\|15}(L)] - 0$	$F_A[x_{A\|9}(L)] - F_A[x_{A\|15}(L)]$
15	8	0			$F_D[x_{D\|8}(L)] - F_D[x_{D\|15}(L)]$	$F_C[x_{C\|15}(L)] - 0$	$F_B[x_{B\|15}(L)] - 0$	$F_A[x_{A\|15}(L)] - 0$

15	7	6	4	0	$F_D[x_{D\|15}(L)] - 0$	$F_C[x_{C\|4}(L)] - F_C[x_{C\|6}(L)]$	$F_B[x_{B\|6}(L)] - F_B[x_{B\|7}(L)]$	$F_A[x_{A\|7}(L)] - F_A[x_{A\|15}(L)]$
15	7	6	2	0	$F_D[x_{D\|15}(L)] - 0$	$F_C[x_{C\|6}(L)] - F_C[x_{C\|7}(L)]$	$F_B[x_{B\|2}(L)] - F_B[x_{B\|6}(L)]$	$F_A[x_{A\|7}(L)] - F_A[x_{A\|15}(L)]$
15	7	6	0		$F_D[x_{D\|15}(L)] - 0$	$F_C[x_{C\|6}(L)] - F_C[x_{C\|7}(L)]$	$F_B[x_{B\|6}(L)] - F_B[x_{B\|7}(L)]$	$F_A[x_{A\|7}(L)] - F_A[x_{A\|15}(L)]$
15	7	5	4	0	$F_D[x_{D\|15}(L)] - 0$	$F_C[x_{C\|4}(L)] - F_C[x_{C\|5}(L)]$	$F_B[x_{B\|7}(L)] - F_B[x_{B\|15}(L)]$	$F_A[x_{A\|5}(L)] - F_A[x_{A\|7}(L)]$
15	7	5	1	0	$F_D[x_{D\|15}(L)] - 0$	$F_C[x_{C\|5}(L)] - F_C[x_{C\|7}(L)]$	$F_B[x_{B\|7}(L)] - F_B[x_{B\|15}(L)]$	$F_A[x_{A\|1}(L)] - F_A[x_{A\|5}(L)]$
15	7	5	0		$F_D[x_{D\|15}(L)] - 0$	$F_C[x_{C\|5}(L)] - F_C[x_{C\|7}(L)]$	$F_B[x_{B\|7}(L)] - F_B[x_{B\|15}(L)]$	$F_A[x_{A\|5}(L)] - F_A[x_{A\|7}(L)]$
15	7	4	0		$F_D[x_{D\|15}(L)] - 0$	$F_C[x_{C\|4}(L)] - F_C[x_{C\|7}(L)]$	$F_B[x_{B\|7}(L)] - F_B[x_{B\|15}(L)]$	$F_A[x_{A\|7}(L)] - F_A[x_{A\|15}(L)]$
15	7	3	2	0	$F_D[x_{D\|15}(L)] - 0$	$F_C[x_{C\|7}(L)] - F_C[x_{C\|15}(L)]$	$F_B[x_{B\|2}(L)] - F_B[x_{B\|3}(L)]$	$F_A[x_{A\|3}(L)] - F_A[x_{A\|7}(L)]$
15	7	3	1	0	$F_D[x_{D\|15}(L)] - 0$	$F_C[x_{C\|7}(L)] - F_C[x_{C\|15}(L)]$	$F_B[x_{B\|3}(L)] - F_B[x_{B\|7}(L)]$	$F_A[x_{A\|1}(L)] - F_A[x_{A\|3}(L)]$
15	7	3	0		$F_D[x_{D\|15}(L)] - 0$	$F_C[x_{C\|7}(L)] - F_C[x_{C\|15}(L)]$	$F_B[x_{B\|3}(L)] - F_B[x_{B\|7}(L)]$	$F_A[x_{A\|3}(L)] - F_A[x_{A\|7}(L)]$
15	7	2	0		$F_D[x_{D\|15}(L)] - 0$	$F_C[x_{C\|7}(L)] - F_C[x_{C\|15}(L)]$	$F_B[x_{B\|2}(L)] - F_B[x_{B\|7}(L)]$	$F_A[x_{A\|7}(L)] - F_A[x_{A\|15}(L)]$
15	7	1	0		$F_D[x_{D\|15}(L)] - 0$	$F_C[x_{C\|7}(L)] - F_C[x_{C\|15}(L)]$	$F_B[x_{B\|7}(L)] - F_B[x_{B\|15}(L)]$	$F_A[x_{A\|1}(L)] - F_A[x_{A\|7}(L)]$
15	7	0			$F_D[x_{D\|15}(L)] - 0$	$F_C[x_{C\|7}(L)] - F_C[x_{C\|15}(L)]$	$F_B[x_{B\|7}(L)] - F_B[x_{B\|15}(L)]$	$F_A[x_{A\|7}(L)] - F_A[x_{A\|15}(L)]$
15	6	4	0		$F_D[x_{D\|15}(L)] - 0$	$F_C[x_{C\|4}(L)] - F_C[x_{C\|6}(L)]$	$F_B[x_{B\|6}(L)] - F_B[x_{B\|15}(L)]$	$F_A[x_{A\|15}(L)] - 0$
15	6	2	0		$F_D[x_{D\|15}(L)] - 0$	$F_C[x_{C\|6}(L)] - F_C[x_{C\|15}(L)]$	$F_B[x_{B\|2}(L)] - F_B[x_{B\|6}(L)]$	$F_A[x_{A\|15}(L)] - 0$
15	6	0			$F_D[x_{D\|15}(L)] - 0$	$F_C[x_{C\|6}(L)] - F_C[x_{C\|15}(L)]$	$F_B[x_{B\|6}(L)] - F_B[x_{B\|15}(L)]$	$F_A[x_{A\|15}(L)] - 0$
15	5	4	0		$F_D[x_{D\|15}(L)] - 0$	$F_C[x_{C\|4}(L)] - F_C[x_{C\|5}(L)]$	$F_B[x_{B\|15}(L)] - 0$	$F_A[x_{A\|5}(L)] - F_A[x_{A\|15}(L)]$
15	5	1	0		$F_D[x_{D\|15}(L)] - 0$	$F_C[x_{C\|5}(L)] - F_C[x_{C\|15}(L)]$	$F_B[x_{B\|15}(L)] - 0$	$F_A[x_{A\|1}(L)] - F_A[x_{A\|5}(L)]$
15	5	0			$F_D[x_{D\|15}(L)] - 0$	$F_C[x_{C\|5}(L)] - F_C[x_{C\|15}(L)]$	$F_B[x_{B\|15}(L)] - 0$	$F_A[x_{A\|5}(L)] - F_A[x_{A\|15}(L)]$
15	4	0			$F_D[x_{D\|15}(L)] - 0$	$F_C[x_{C\|4}(L)] - F_C[x_{C\|15}(L)]$	$F_B[x_{B\|15}(L)] - 0$	$F_A[x_{A\|15}(L)] - 0$
15	3	2	0		$F_D[x_{D\|15}(L)] - 0$	$F_C[x_{C\|15}(L)] - 0$	$F_B[x_{B\|2}(L)] - F_B[x_{B\|3}(L)]$	$F_A[x_{A\|3}(L)] - F_A[x_{A\|15}(L)]$
15	3	1	0		$F_D[x_{D\|15}(L)] - 0$	$F_C[x_{C\|15}(L)] - 0$	$F_B[x_{B\|3}(L)] - F_B[x_{B\|15}(L)]$	$F_A[x_{A\|1}(L)] - F_A[x_{A\|3}(L)]$
15	3	0			$F_D[x_{D\|15}(L)] - 0$	$F_C[x_{C\|15}(L)] - 0$	$F_B[x_{B\|3}(L)] - F_B[x_{B\|15}(L)]$	$F_A[x_{A\|3}(L)] - F_A[x_{A\|15}(L)]$
15	2	0			$F_D[x_{D\|15}(L)] - 0$	$F_C[x_{C\|15}(L)] - 0$	$F_B[x_{B\|2}(L)] - F_B[x_{B\|15}(L)]$	$F_A[x_{A\|15}(L)] - 0$

15	1	0	$F_D[x_{D\|15}(L)] - 0$	$F_C[x_{C\|15}(L)] - 0$	$F_B[x_{B\|15}(L)] - 0$	$F_A[x_{A\|1}(L)] - F_A[x_{A\|15}(L)]$
15	0		$F_D[x_{D\|15}(L)] - 0$	$F_C[x_{C\|15}(L)] - 0$	$F_B[x_{B\|15}(L)] - 0$	$F_A[x_{A\|15}(L)] - 0$

Note: The difference between the probabilty of a state is not the same as the transitional state. Note e.g. 8 (C-1) of table 1; 15 14 12 8 and the 8 for (C-1) of table 2 ;15,13, 12,8 are different. The state implies ergodic (Markov) whereas the transitional state is path dependent but with fading memeory, i.e. it depends only on the two most recent state.

TABLE 2. PROBABILITY OF TOTAL SYSTEM FAILURE GIVEN ONE COMPONENT FAILED

Failure Sequences	Probability of Failure of Component $L \leq L$			
	D	C	B	A
14 12 8 0	$F_D[x_{D\|8}(L)] - F_D[x_{D\|12}(L)]$	$F_C[x_{C\|12}(L)] - F_C[x_{C\|14}(L)]$	$F_B[x_{B\|14}(L)] - F_B[x_{B\|15}(L)]$	
14 12 4 0	$F_D[x_{D\|12}(L)] - F_D[x_{D\|14}(L)]$	$F_C[x_{C\|4}(L)] - F_C[x_{C\|12}(L)]$	$F_B[x_{B\|14}(L)] - F_B[x_{B\|15}(L)]$	
14 12 0	$F_D[x_{D\|12}(L)] - F_D[x_{D\|14}(L)]$	$F_C[x_{C\|12}(L)] - F_C[x_{C\|14}(L)]$	$F_B[x_{B\|14}(L)] - F_B[x_{B\|15}(L)]$	
14 10 8 0	$F_D[x_{D\|8}(L)] - F_D[x_{D\|10}(L)]$	$F_C[x_{C\|14}(L)] - F_C[x_{C\|15}(L)]$	$F_B[x_{B\|10}(L)] - F_B[x_{B\|14}(L)]$	
14 10 2 0	$F_D[x_{D\|10}(L)] - F_D[x_{D\|14}(L)]$	$F_C[x_{C\|14}(L)] - F_C[x_{C\|15}(L)]$	$F_B[x_{B\|2}(L)] - F_B[x_{B\|10}(L)]$	
14 10 0	$F_D[x_{D\|10}(L)] - F_D[x_{D\|14}(L)]$	$F_C[x_{C\|14}(L)] - F_C[x_{C\|15}(L)]$	$F_B[x_{B\|10}(L)] - F_B[x_{B\|14}(L)]$	
14 8 0	$F_D[x_{D\|8}(L)] - F_D[x_{D\|14}(L)]$	$F_C[x_{C\|14}(L)] - F_C[x_{C\|15}(L)]$	$F_B[x_{B\|14}(L)] - F_B[x_{B\|15}(L)]$	
14 6 4 0	$F_D[x_{D\|14}(L)] - F_D[x_{D\|15}(L)]$	$F_C[x_{C\|4}(L)] - F_C[x_{C\|6}(L)]$	$F_B[x_{B\|6}(L)] - F_B[x_{B\|14}(L)]$	
14 6 2 0	$F_D[x_{D\|14}(L)] - F_D[x_{D\|15}(L)]$	$F_C[x_{C\|6}(L)] - F_C[x_{C\|14}(L)]$	$F_B[x_{B\|2}(L)] - F_B[x_{B\|6}(L)]$	
14 6 0	$F_D[x_{D\|14}(L)] - F_D[x_{D\|15}(L)]$	$F_C[x_{C\|6}(L)] - F_C[x_{C\|14}(L)]$	$F_B[x_{B\|6}(L)] - F_B[x_{B\|14}(L)]$	
14 4 0	$F_D[x_{D\|14}(L)] - F_D[x_{D\|15}(L)]$	$F_C[x_{C\|4}(L)] - F_C[x_{C\|14}(L)]$	$F_B[x_{B\|14}(L)] - F_B[x_{B\|15}(L)]$	
14 2 0	$F_D[x_{D\|14}(L)] - F_D[x_{D\|15}(L)]$	$F_C[x_{C\|14}(L)] - F_C[x_{C\|15}(L)]$	$F_B[x_{B\|2}(L)] - F_B[x_{B\|14}(L)]$	
14 0	$F_D[x_{D\|14}(L)] - F_D[x_{D\|15}(L)]$	$F_C[x_{C\|14}(L)] - F_C[x_{C\|15}(L)]$	$F_B[x_{B\|14}(L)] - F_B[x_{B\|15}(L)]$	
13 12 8 0	$F_D[x_{D\|8}(L)] - F_D[x_{D\|12}(L)$	$F_C[x_{C\|13}(L)] - F_C[x_{C\|12}(L)]$		$F_A[x_{A\|13}(L)] - F_A[x_{A\|15}(L)]$
13 12 4 0	$F_D[x_{D\|13}(L)] - F_D[x_{D\|12}(L)]$	$F_C[x_{C\|4}(L)] - F_C[x_{C\|12}(L)]$		$F_A[x_{A\|13}(L)] - F_A[x_{A\|15}(L)]$
13 12 0	$F_D[x_{D\|13}(L)] - F_D[x_{D\|12}(L)]$	$F_C[x_{C\|13}(L)] - F_C[x_{C\|12}(L)]$		$F_A[x_{A\|13}(L)] - F_A[x_{A\|15}(L)]$
13 9 8 0	$F_D[x_{D\|8}(L)] - F_D[x_{D\|9}(L)]$	$F_C[x_{C\|13}(L)] - F_C[x_{C\|15}(L)]$		$F_A[x_{A\|9}(L)] - F_A[x_{A\|13}(L)]$
13 9 1 0	$F_D[x_{D\|9}(L)] - F_D[x_{D\|13}(L)]$	$F_C[x_{C\|13}(L)] - F_C[x_{C\|15}(L)]$		$F_A[x_{A\|1}(L)] - F_A[x_{A\|9}(L)]$
13 9 0	$F_D[x_{D\|9}(L)] - F_D[x_{D\|13}(L)]$	$F_C[x_{C\|13}(L)] - F_C[x_{C\|15}(L)]$		$F_A[x_{A\|9}(L)] - F_A[x_{A\|13}(L)]$
13 8 0	$F_D[x_{D\|8}(L)] - F_D[x_{D\|13}(L)]$	$F_C[x_{C\|13}(L)] - F_C[x_{C\|15}(L)]$		$F_A[x_{A\|13}(L)] - F_A[x_{A\|15}(L)]$
13 5 4 0	$F_D[x_{D\|13}(L)] - F_D[x_{D\|15}(L)]$	$F_C[x_{C\|4}(L)] - F_C[x_{C\|5}(L)]$		$F_A[x_{A\|5}(L)] - F_A[x_{A\|13}(L)]$
13 5 1 0	$F_D[x_{D\|13}(L)] - F_D[x_{D\|15}(L)]$	$F_C[x_{C\|5}(L)] - F_C[x_{C\|13}(L)]$		$F_A[x_{A\|1}(L)] - F_A[x_{A\|5}(L)]$
13 5 0	$F_D[x_{D\|13}(L)] - F_D[x_{D\|15}(L)]$	$F_C[x_{C\|5}(L)] - F_C[x_{C\|13}(L)]$		$F_A[x_{A\|5}(L)] - F_A[x_{A\|13}(L)]$
13 4 0	$F_D[x_{D\|13}(L)] - F_D[x_{D\|15}(L)]$	$F_C[x_{C\|4}(L)] - F_C[x_{C\|13}(L)]$		$F_A[x_{A\|13}(L)] - F_A[x_{A\|15}(L)]$
13 1 0	$F_D[x_{D\|13}(L)] - F_D[x_{D\|15}(L)]$	$F_C[x_{C\|13}(L)] - F_C[x_{C\|15}(L)]$		$F_A[x_{A\|1}(L)] - F_A[x_{A\|13}(L)]$
13 0	$F_D[x_{D\|13}(L)] - F_D[x_{D\|15}(L)]$	$F_C[x_{C\|13}(L)] - F_C[x_{C\|15}(L)]$		$F_A[x_{A\|13}(L)] - F_A[x_{A\|15}(L)]$

11	10	8	0	$F_D[x_{D\|8}(L)] - F_D[x_{D\|10}(L)]$		$F_B[x_{B\|10}(L)] - F_B[x_{B\|11}(L)]$	$F_A[x_{A\|11}(L)] - F_A[x_{A\|15}(L)]$
11	10	2	0	$F_D[x_{D\|10}(L)] - F_D[x_{D\|11}(L)]$		$F_B[x_{B\|2}(L)] - F_B[x_{B\|10}(L)]$	$F_A[x_{A\|11}(L)] - F_A[x_{A\|15}(L)]$
11	10	0		$F_D[x_{D\|10}(L)] - F_D[x_{D\|11}(L)]$		$F_B[x_{B\|10}(L)] - F_B[x_{B\|11}(L)]$	$F_A[x_{A\|11}(L)] - F_A[x_{A\|15}(L)]$
11	9	8	0	$F_D[x_{D\|8}(L)] - F_D[x_{D\|9}(L)]$		$F_B[x_{B\|11}(L)] - F_B[x_{B\|15}(L)]$	$F_A[x_{A\|9}(L)] - F_A[x_{A\|11}(L)]$
11	9	1	0	$F_D[x_{D\|9}(L)] - F_D[x_{D\|11}(L)]$		$F_B[x_{B\|11}(L)] - F_B[x_{B\|15}(L)]$	$F_A[x_{A\|1}(L)] - F_A[x_{A\|9}(L)]$
11	9	0		$F_D[x_{D\|9}(L)] - F_D[x_{D\|11}(L)]$		$F_B[x_{B\|11}(L)] - F_B[x_{B\|15}(L)]$	$F_A[x_{A\|9}(L)] - F_A[x_{A\|11}(L)]$
11	8	0		$F_D[x_{D\|8}(L)] - F_D[x_{D\|11}(L)]$		$F_B[x_{B\|11}(L)] - F_B[x_{B\|15}(L)]$	$F_A[x_{A\|11}(L)] - F_A[x_{A\|15}(L)]$
11	3	2	0	$F_D[x_{D\|11}(L)] - F_D[x_{D\|15}(L)]$		$F_B[x_{B\|2}(L)] - F_B[x_{B\|3}(L)]$	$F_A[x_{A\|3}(L)] - F_A[x_{A\|11}(L)]$
11	3	1	0	$F_D[x_{D\|11}(L)] - F_D[x_{D\|15}(L)]$		$F_B[x_{B\|3}(L)] - F_B[x_{B\|11}(L)]$	$F_A[x_{A\|1}(L)] - F_A[x_{A\|3}(L)]$
11	3	0		$F_D[x_{D\|11}(L)] - F_D[x_{D\|15}(L)]$		$F_B[x_{B\|3}(L)] - F_B[x_{B\|11}(L)]$	$F_A[x_{A\|3}(L)] - F_A[x_{A\|11}(L)]$
11	2	0		$F_D[x_{D\|11}(L)] - F_D[x_{D\|15}(L)]$		$F_B[x_{B\|2}(L)] - F_B[x_{B\|11}(L)]$	$F_A[x_{A\|11}(L)] - F_A[x_{A\|15}(L)]$
11	1	0		$F_D[x_{D\|11}(L)] - F_D[x_{D\|15}(L)]$		$F_B[x_{B\|11}(L)] - F_B[x_{B\|15}(L)]$	$F_A[x_{A\|1}(L)] - F_A[x_{A\|11}(L)]$
11	0			$F_D[x_{D\|11}(L)] - F_D[x_{D\|15}(L)]$		$F_B[x_{B\|11}(L)] - F_B[x_{B\|15}(L)]$	$F_A[x_{A\|11}(L)] - F_A[x_{A\|15}(L)]$
7	6	4	0		$F_C[x_{C\|4}(L)] - F_C[x_{C\|6}(L)]$	$F_B[x_{B\|6}(L)] - F_B[x_{B\|7}(L)]$	$F_A[x_{A\|7}(L)] - F_A[x_{A\|15}(L)]$
7	6	2	0		$F_C[x_{C\|6}(L)] - F_C[x_{C\|7}(L)]$	$F_B[x_{B\|2}(L)] - F_B[x_{B\|6}(L)]$	$F_A[x_{A\|7}(L)] - F_A[x_{A\|15}(L)]$
7	6	0			$F_C[x_{C\|6}(L)] - F_C[x_{C\|7}(L)]$	$F_B[x_{B\|6}(L)] - F_B[x_{B\|7}(L)]$	$F_A[x_{A\|7}(L)] - F_A[x_{A\|15}(L)]$
7	5	4	0		$F_C[x_{C\|4}(L)] - F_C[x_{C\|5}(L)]$	$F_B[x_{B\|7}(L)] - F_B[x_{B\|15}(L)]$	$F_A[x_{A\|5}(L)] - F_A[x_{A\|7}(L)]$
7	5	1	0		$F_C[x_{C\|5}(L)] - F_C[x_{C\|7}(L)]$	$F_B[x_{B\|7}(L)] - F_B[x_{B\|15}(L)]$	$F_A[x_{A\|1}(L)] - F_A[x_{A\|5}(L)]$
7	5	0			$F_C[x_{C\|5}(L)] - F_C[x_{C\|7}(L)]$	$F_B[x_{B\|7}(L)] - F_B[x_{B\|15}(L)]$	$F_A[x_{A\|5}(L)] - F_A[x_{A\|7}(L)]$
7	4	0			$F_C[x_{C\|4}(L)] - F_C[x_{C\|7}(L)]$	$F_B[x_{B\|7}(L)] - F_B[x_{B\|15}(L)]$	$F_A[x_{A\|7}(L)] - F_A[x_{A\|15}(L)]$
7	3	2	0		$F_C[x_{C\|7}(L)] - F_C[x_{C\|15}(L)]$	$F_B[x_{B\|2}(L)] - F_B[x_{B\|3}(L)]$	$F_A[x_{A\|3}(L)] - F_A[x_{A\|7}(L)]$
7	3	1	0		$F_C[x_{C\|7}(L)] - F_C[x_{C\|15}(L)]$	$F_B[x_{B\|3}(L)] - F_B[x_{B\|7}(L)]$	$F_A[x_{A\|1}(L)] - F_A[x_{A\|3}(L)]$
7	3	0			$F_C[x_{C\|7}(L)] - F_C[x_{C\|15}(L)]$	$F_B[x_{B\|3}(L)] - F_B[x_{B\|7}(L)]$	$F_A[x_{A\|3}(L)] - F_A[x_{A\|7}(L)]$
7	2	0			$F_C[x_{C\|7}(L)] - F_C[x_{C\|15}(L)]$	$F_B[x_{B\|2}(L)] - F_B[x_{B\|7}(L)]$	$F_A[x_{A\|7}(L)] - F_A[x_{A\|15}(L)]$
7	1	0			$F_C[x_{C\|7}(L)] - F_C[x_{C\|15}(L)]$	$F_B[x_{B\|7}(L)] - F_B[x_{B\|15}(L)]$	$F_A[x_{A\|1}(L)] - F_A[x_{A\|7}(L)]$
7	0				$F_C[x_{C\|7}(L)] - F_C[x_{C\|15}(L)]$	$F_B[x_{B\|7}(L)] - F_B[x_{B\|15}(L)]$	$F_A[x_{A\|7}(L)] - F_A[x_{A\|15}(L)]$

TABLE 3. PROBABILITY OF TOTAL SYSTEM FAILURE GIVEN TWO COMPONENTS FAILED

Failure Sequences			Probability of Failure of Component L ≤ L			
			D	C	B	A
12	8	0	$F_D[x_{D\|8}(L)] - F_D[x_{D\|12}(L)]$	$F_C[x_{C\|12}(L)] - F_C[x_{C\|14}(L)]$		
12	4	0	$F_D[x_{D\|12}(L)] - F_D[x_{D\|14}(L)]$	$F_C[x_{C\|4}(L)] - F_C[x_{C\|12}(L)]$		
12	0		$F_D[x_{D\|12}(L)] - F_D[x_{D\|14}(L)]$	$F_C[x_{C\|12}(L)] - F_C[x_{C\|14}(L)]$		
10	8	0	$F_D[x_{D\|8}(L)] - F_D[x_{D\|10}(L)]$		$F_B[x_{B\|10}(L)] - F_B[x_{B\|14}(L)]$	
10	2	0	$F_D[x_{D\|10}(L)] - F_D[x_{D\|14}(L)]$		$F_B[x_{B\|2}(L)] - F_B[x_{B\|10}(L)]$	
10	0		$F_D[x_{D\|10}(L)] - F_D[x_{D\|14}(L)]$		$F_B[x_{B\|10}(L)] - F_B[x_{B\|14}(L)]$	
6	4	0		$F_C[x_{C\|4}(L)] - F_C[x_{C\|6}(L)]$	$F_B[x_{B\|6}(L)] - F_B[x_{B\|14}(L)]$	
6	2	0		$F_C[x_{C\|6}(L)] - F_C[x_{C\|14}(L)]$	$F_B[x_{B\|2}(L)] - F_B[x_{B\|6}(L)]$	
6	0			$F_C[x_{C\|6}(L)] - F_C[x_{C\|14}(L)]$	$F_B[x_{B\|6}(L)] - F_B[x_{B\|14}(L)]$	
12	8	0	$F_D[x_{D\|8}(L)] - F_D[x_{D\|12}(L)$	$F_C[x_{C\|13}(L)] - F_C[x_{C\|12}(L)]$		
12	4	0	$F_D[x_{D\|13}(L)] - F_D[x_{D\|12}(L)]$	$F_C[x_{C\|4}(L)] - F_C[x_{C\|12}(L)]$		
12	0		$F_D[x_{D\|13}(L)] - F_D[x_{D\|12}(L)]$	$F_C[x_{C\|13}(L)] - F_C[x_{C\|12}(L)]$		
9	8	0	$F_D[x_{D\|8}(L)] - F_D[x_{D\|9}(L)]$			$F_A[x_{A\|9}(L)] - F_A[x_{A\|13}(L)]$
9	1	0	$F_D[x_{D\|9}(L)] - F_D[x_{D\|13}(L)]$			$F_A[x_{A\|1}(L)] - F_A[x_{A\|9}(L)]$
9	0		$F_D[x_{D\|9}(L)] - F_D[x_{D\|13}(L)]$			$F_A[x_{A\|9}(L)] - F_A[x_{A\|13}(L)]$
5	4	0		$F_C[x_{C\|4}(L)] - F_C[x_{C\|5}(L)]$		$F_A[x_{A\|5}(L)] - F_A[x_{A\|13}(L)]$
5	1	0		$F_C[x_{C\|5}(L)] - F_C[x_{C\|13}(L)]$		$F_A[x_{A\|1}(L)] - F_A[x_{A\|5}(L)]$
5	0			$F_C[x_{C\|5}(L)] - F_C[x_{C\|13}(L)]$		$F_A[x_{A\|5}(L)] - F_A[x_{A\|13}(L)]$
12	8	0	$F_D[x_{D\|8}(L)] - F_D[x_{D\|12}(L)]$	$F_C[x_{C\|12}(L)] - F_C[x_{C\|15}(L)]$		
12	4	0	$F_D[x_{D\|12}(L)] - F_D[x_{D\|15}(L)]$	$F_C[x_{C\|4}(L)] - F_C[x_{C\|12}(L)]$		
12	0		$F_D[x_{D\|12}(L)] - F_D[x_{D\|15}(L)]$	$F_C[x_{C\|12}(L)] - F_C[x_{C\|15}(L)]$		
10	8	0	$F_D[x_{D\|8}(L)] - F_D[x_{D\|10}(L)]$		$F_B[x_{B\|10}(L)] - F_B[x_{B\|11}(L)]$	
10	2	0	$F_D[x_{D\|10}(L)] - F_D[x_{D\|11}(L)]$		$F_B[x_{B\|2}(L)] - F_B[x_{B\|10}(L)]$	
10	0		$F_D[x_{D\|10}(L)] - F_D[x_{D\|11}(L)]$		$F_B[x_{B\|10}(L)] - F_B[x_{B\|11}(L)]$	

9	8	0	$F_D[x_{D\|8}(L)] - F_D[x_{D\|9}(L)]$			$F_A[x_{A\|9}(L)] - F_A[x_{A\|11}(L)]$
9	1	0	$F_D[x_{D\|9}(L)] - F_D[x_{D\|11}(L)]$			$F_A[x_{A\|1}(L)] - F_A[x_{A\|9}(L)]$
9	0		$F_D[x_{D\|9}(L)] - F_D[x_{D\|11}(L)]$			$F_A[x_{A\|9}(L)] - F_A[x_{A\|11}(L)]$
3	2	0			$F_B[x_{B\|2}(L)] - F_B[x_{B\|3}(L)]$	$F_A[x_{A\|3}(L)] - F_A[x_{A\|11}(L)]$
3	1	0			$F_B[x_{B\|3}(L)] - F_B[x_{B\|11}(L)]$	$F_A[x_{A\|1}(L)] - F_A[x_{A\|3}(L)]$
3	0				$F_B[x_{B\|3}(L)] - F_B[x_{B\|11}(L)]$	$F_A[x_{A\|3}(L)] - F_A[x_{A\|11}(L)]$
10	8	0	$F_D[x_{D\|8}(L)] - F_D[x_{D\|10}(L)]$		$F_B[x_{B\|10}(L)] - F_B[x_{B\|15}(L)]$	
10	2	0	$F_D[x_{D\|10}(L)] - F_D[x_{D\|15}(L)]$		$F_B[x_{B\|2}(L)] - F_B[x_{B\|10}(L)]$	
10	0		$F_D[x_{D\|10}(L)] - F_D[x_{D\|15}(L)]$		$F_B[x_{B\|10}(L)] - F_B[x_{B\|15}(L)]$	
9	8	0	$F_D[x_{D\|8}(L)] - F_D[x_{D\|9}(L)]$			$F_A[x_{A\|9}(L)] - F_A[x_{A\|15}(L)]$
9	1	0	$F_D[x_{D\|9}(L)] - F_D[x_{D\|15}(L)]$			$F_A[x_{A\|1}(L)] - F_A[x_{A\|9}(L)]$
9	0		$F_D[x_{D\|9}(L)] - F_D[x_{D\|15}(L)]$			$F_A[x_{A\|9}(L)] - F_A[x_{A\|15}(L)]$
6	4	0		$F_C[x_{C\|4}(L)] - F_C[x_{C\|6}(L)]$	$F_B[x_{B\|6}(L)] - F_B[x_{B\|7}(L)]$	
6	2	0		$F_C[x_{C\|6}(L)] - F_C[x_{C\|7}(L)]$	$F_B[x_{B\|2}(L)] - F_B[x_{B\|6}(L)]$	
6	0			$F_C[x_{C\|6}(L)] - F_C[x_{C\|7}(L)]$	$F_B[x_{B\|6}(L)] - F_B[x_{B\|7}(L)]$	
5	4	0		$F_C[x_{C\|4}(L)] - F_C[x_{C\|5}(L)]$		$F_A[x_{A\|5}(L)] - F_A[x_{A\|7}(L)]$
5	1	0		$F_C[x_{C\|5}(L)] - F_C[x_{C\|7}(L)]$		$F_A[x_{A\|1}(L)] - F_A[x_{A\|5}(L)]$
5	0			$F_C[x_{C\|5}(L)] - F_C[x_{C\|7}(L)]$		$F_A[x_{A\|5}(L)] - F_A[x_{A\|7}(L)]$
3	2	0			$F_B[x_{B\|2}(L)] - F_B[x_{B\|3}(L)]$	$F_A[x_{A\|3}(L)] - F_A[x_{A\|7}(L)]$
3	1	0			$F_B[x_{B\|3}(L)] - F_B[x_{B\|7}(L)]$	$F_A[x_{A\|1}(L)] - F_A[x_{A\|3}(L)]$
3	0				$F_B[x_{B\|3}(L)] - F_B[x_{B\|7}(L)]$	$F_A[x_{A\|3}(L)] - F_A[x_{A\|7}(L)]$
6	4	0		$F_C[x_{C\|4}(L)] - F_C[x_{C\|6}(L)]$	$F_B[x_{B\|6}(L)] - F_B[x_{B\|15}(L)]$	
6	2	0		$F_C[x_{C\|6}(L)] - F_C[x_{C\|15}(L)]$	$F_B[x_{B\|2}(L)] - F_B[x_{B\|6}(L)]$	
6	0			$F_C[x_{C\|6}(L)] - F_C[x_{C\|15}(L)]$	$F_B[x_{B\|6}(L)] - F_B[x_{B\|15}(L)]$	

5	4	0	$F_C[x_{C\|4}(L)] - F_C[x_{C\|5}(L)]$		$F_A[x_{A\|5}(L)] - F_A[x_{A\|15}(L)]$
5	1	0	$F_C[x_{C\|5}(L)] - F_C[x_{C\|15}(L)]$		$F_A[x_{A\|1}(L)] - F_A[x_{A\|5}(L)]$
5	0		$F_C[x_{C\|5}(L)] - F_C[x_{C\|15}(L)]$		$F_A[x_{A\|5}(L)] - F_A[x_{A\|15}(L)]$
3	2	0		$F_B[x_{B\|2}(L)] - F_B[x_{B\|3}(L)]$	$F_A[x_{A\|3}(L)] - F_A[x_{A\|15}(L)]$
3	1	0		$F_B[x_{B\|3}(L)] - F_B[x_{B\|15}(L)]$	$F_A[x_{A\|1}(L)] - F_A[x_{A\|3}(L)]$
3	0			$F_B[x_{B\|3}(L)] - F_B[x_{B\|15}(L)]$	$F_A[x_{A\|3}(L)] - F_A[x_{A\|15}(L)]$

TABLE 4. PROBABILITY OF TOTAL SYSTEM FAILURE GIVEN THREE COMPONENTS FAILED

Failure Sequences		Probability of Failure of Component L ≤ L			
		D	C	B	A
8	0	$F_D[x_{D\|8}(L)] - F_D[x_{D\|12}(L)]$			
4	0		$F_C[x_{C\|4}(L)] - F_C[x_{C\|12}(L)]$		
8	0	$F_D[x_{D\|8}(L)] - F_D[x_{D\|10}(L)]$			
2	0			$F_B[x_{B\|2}(L)] - F_B[x_{B\|10}(L)]$	
8	0	$F_D[x_{D\|8}(L)] - F_D[x_{D\|14}(L)]$			
4	0		$F_C[x_{C\|4}(L)] - F_C[x_{C\|6}(L)]$		
2	0			$F_B[x_{B\|2}(L)] - F_B[x_{B\|6}(L)]$	
4	0		$F_C[x_{C\|4}(L)] - F_C[x_{C\|14}(L)]$		
2	0			$F_B[x_{B\|2}(L)] - F_B[x_{B\|14}(L)]$	
8	0	$F_D[x_{D\|8}(L)] - F_D[x_{D\|12}(L)$			
4	0		$F_C[x_{C\|4}(L)] - F_C[x_{C\|12}(L)]$		
8	0	$F_D[x_{D\|8}(L)] - F_D[x_{D\|9}(L)]$			
1	0				$F_A[x_{A\|9}(L)] - F_A[x_{A\|1}(L)]$
8	0	$F_D[x_{D\|8}(L)] - F_D[x_{D\|13}(L)]$			
4	0		$F_C[x_{C\|4}(L)] - F_C[x_{C\|5}(L)]$		
1	0				$F_A[x_{A\|1}(L)] - F_A[x_{A\|5}(L)]$
4	0		$F_C[x_{C\|4}(L)] - F_C[x_{C\|13}(L)]$		
1	0				$F_A[x_{A\|1}(L)] - F_A[x_{A\|13}(L)]$
8	0	$F_D[x_{D\|8}(L)] - F_D[x_{D\|12}(L)]$			
4	0		$F_C[x_{C\|4}(L)] - F_C[x_{C\|12}(L)]$		
8	0	$F_D[x_{D\|8}(L)] - F_D[x_{D\|10}(L)]$			
2	0			$F_B[x_{B\|2}(L)] - F_B[x_{B\|10}(L)]$	
8	0	$F_D[x_{D\|8}(L)] - F_D[x_{D\|9}(L)]$			
1	0				$F_A[x_{A\|1}(L)] - F_A[x_{A\|9}(L)]$

8	0	$F_D[x_{D\|8}(L)] - F_D[x_{D\|11}(L)]$			
2	0			$F_B[x_{B\|2}(L)] - F_B[x_{B\|3}(L)]$	
1	0				$F_A[x_{A\|1}(L)] - F_A[x_{A\|3}(L)]$
2	0			$F_B[x_{B\|2}(L)] - F_B[x_{B\|3}(L)]$	
1	0				$F_A[x_{A\|1}(L)] - F_A[x_{A\|3}(L)]$
8	0	$F_D[x_{D\|8}(L)] - F_D[x_{D\|10}(L)]$			
2	0			$F_B[x_{B\|2}(L)] - F_B[x_{B\|10}(L)]$	
8	0	$F_D[x_{D\|8}(L)] - F_D[x_{D\|9}(L)]$			
1	0				$F_A[x_{A\|1}(L)] - F_A[x_{A\|9}(L)]$
8	0	$F_D[x_{D\|8}(L)] - F_D[x_{D\|15}(L)]$			
4	0		$F_C[x_{C\|4}(L)] - F_C[x_{C\|6}(L)]$		
2	0			$F_B[x_{B\|2}(L)] - F_B[x_{B\|6}(L)]$	
4	0		$F_C[x_{C\|4}(L)] - F_C[x_{C\|5}(L)]$		
1	0				$F_A[x_{A\|1}(L)] - F_A[x_{A\|5}(L)]$
4	0		$F_C[x_{C\|4}(L)] - F_C[x_{C\|7}(L)]$		
2	0			$F_B[x_{B\|2}(L)] - F_B[x_{B\|3}(L)]$	
1	0				$F_A[x_{A\|1}(L)] - F_A[x_{A\|3}(L)]$
2	0			$F_B[x_{B\|2}(L)] - F_B[x_{B\|7}(L)]$	
1	0				$F_A[x_{A\|1}(L)] - F_A[x_{A\|7}(L)]$
4	0		$F_C[x_{C\|4}(L)] - F_C[x_{C\|6}(L)]$		
2	0			$F_B[x_{B\|2}(L)] - F_B[x_{B\|6}(L)]$	
4	0		$F_C[x_{C\|4}(L)] - F_C[x_{C\|5}(L)]$		
1	0				$F_A[x_{A\|1}(L)] - F_A[x_{A\|5}(L)]$
4	0		$F_C[x_{C\|4}(L)] - F_C[x_{C\|15}(L)]$		

2	0	$F_B[x_{B\|2}(L)] - F_B[x_{B\|3}(L)]$	
1	0		$F_A[x_{A\|1}(L)] - F_A[x_{A\|3}(L)]$
2	0	$F_B[x_{B\|2}(L)] - F_B[x_{B\|15}(L)]$	
1	0		$F_A[x_{A\|1}(L)] - F_A[x_{A\|15}(L)]$

TABLE 5. PROBABILITY OF TWO COMPONENT FAILURE GIVEN ONE COMPONENT FAILED

Failure Sequences		Probability of Failure of Component $L \leq L$			
		D	C	B	A
14	12			$F_B[x_{B\|14}(L)] - F_B[x_{B\|15}(L)]$	
14	12			$F_B[x_{B\|14}(L)] - F_B[x_{B\|15}(L)]$	
14	12			$F_B[x_{B\|14}(L)] - F_B[x_{B\|15}(L)]$	
14	10	$F_D[x_{D\|8}(L)] - F_D[x_{D\|10}(L)]$	$F_C[x_{C\|14}(L)] - F_C[x_{C\|15}(L)]$		
14	10	$F_D[x_{D\|10}(L)] - F_D[x_{D\|14}(L)]$	$F_C[x_{C\|14}(L)] - F_C[x_{C\|15}(L)]$		
14	10	$F_D[x_{D\|10}(L)] - F_D[x_{D\|14}(L)]$	$F_C[x_{C\|14}(L)] - F_C[x_{C\|15}(L)]$		
14	6	$F_D[x_{D\|14}(L)] - F_D[x_{D\|15}(L)]$			
14	6	$F_D[x_{D\|14}(L)] - F_D[x_{D\|15}(L)]$			
14	6	$F_D[x_{D\|14}(L)] - F_D[x_{D\|15}(L)]$			
13	12				$F_A[x_{A\|13}(L)] - F_A[x_{A\|15}(L)]$
13	12				$F_A[x_{A\|13}(L)] - F_A[x_{A\|15}(L)]$
13	12				$F_A[x_{A\|13}(L)] - F_A[x_{A\|15}(L)]$
13	9		$F_C[x_{C\|13}(L)] - F_C[x_{C\|15}(L)]$		
13	9		$F_C[x_{C\|13}(L)] - F_C[x_{C\|15}(L)]$		
13	9		$F_C[x_{C\|13}(L)] - F_C[x_{C\|15}(L)]$		
13	5	$F_D[x_{D\|13}(L)] - F_D[x_{D\|15}(L)]$			
13	5	$F_D[x_{D\|13}(L)] - F_D[x_{D\|15}(L)]$			
13	5	$F_D[x_{D\|13}(L)] - F_D[x_{D\|15}(L)]$			
11	10				$F_A[x_{A\|11}(L)] - F_A[x_{A\|15}(L)]$
11	10				$F_A[x_{A\|11}(L)] - F_A[x_{A\|15}(L)]$
11	10				$F_A[x_{A\|11}(L)] - F_A[x_{A\|15}(L)]$
11	9			$F_B[x_{B\|11}(L)] - F_B[x_{B\|15}(L)]$	
11	9			$F_B[x_{B\|11}(L)] - F_B[x_{B\|15}(L)]$	
11	9			$F_B[x_{B\|11}(L)] - F_B[x_{B\|15}(L)]$	
11	3	$F_D[x_{D\|11}(L)] - F_D[x_{D\|15}(L)]$			

11	3	$F_D[x_{D\|11}\ (L)] - F_D[x_{D\|15}\ (L)]$			
11	3	$F_D[x_{D\|11}\ (L)] - F_D[x_{D\|15}\ (L)]$			
7	6				$F_A[x_{A\|7}\ (L)] - F_A[x_{A\|15}\ (L)]$
7	6				$F_A[x_{A\|7}\ (L)] - F_A[x_{A\|15}\ (L)]$
7	6				$F_A[x_{A\|7}\ (L)] - F_A[x_{A\|15}\ (L)]$
7	5			$F_B[x_{B\|7}\ (L)] - F_B[x_{B\|15}\ (L)]$	
7	5			$F_B[x_{B\|7}\ (L)] - F_B[x_{B\|15}\ (L)]$	
7	5			$F_B[x_{B\|7}\ (L)] - F_B[x_{B\|15}\ (L)]$	
7	3		$F_C[x_{C\|7}(L)] - F_C[x_{C\|15}\ (L)]$		
7	3		$F_C[x_{C\|7}(L)] - F_C[x_{C\|15}\ (L)]$		
7	3		$F_C[x_{C\|7}(L)] - F_C[x_{C\|15}\ (L)]$		

TABLE 6. PROBABILITY OF THREE COMPONENT FAILURE GIVEN ONE COMPONENT FAILED

Failure Sequences			Probability of Failure of Component L ≤ L			
			D	C	B	A
14	12	8		$F_C[x_{C\|12}(L)] - F_C[x_{C\|14}(L)]$	$F_B[x_{B\|14}(L)] - F_B[x_{B\|15}(L)]$	
14	12	4	$F_D[x_{D\|12}(L)] - F_D[x_{D\|14}(L)]$		$F_B[x_{B\|14}(L)] - F_B[x_{B\|15}(L)]$	
14	10	8		$F_C[x_{C\|14}(L)] - F_C[x_{C\|15}(L)]$	$F_B[x_{B\|10}(L)] - F_B[x_{B\|14}(L)]$	
14	10	2	$F_D[x_{D\|10}(L)] - F_D[x_{D\|14}(L)]$	$F_C[x_{C\|14}(L)] - F_C[x_{C\|15}(L)]$		
14	8			$F_C[x_{C\|14}(L)] - F_C[x_{C\|15}(L)]$	$F_B[x_{B\|14}(L)] - F_B[x_{B\|15}(L)]$	
14	6	4	$F_D[x_{D\|14}(L)] - F_D[x_{D\|15}(L)]$		$F_B[x_{B\|6}(L)] - F_B[x_{B\|14}(L)]$	
14	6	2	$F_D[x_{D\|14}(L)] - F_D[x_{D\|15}(L)]$	$F_C[x_{C\|6}(L)] - F_C[x_{C\|14}(L)]$		
14	4		$F_D[x_{D\|14}(L)] - F_D[x_{D\|15}(L)]$		$F_B[x_{B\|14}(L)] - F_B[x_{B\|15}(L)]$	
14	2		$F_D[x_{D\|14}(L)] - F_D[x_{D\|15}(L)]$	$F_C[x_{C\|14}(L)] - F_C[x_{C\|15}(L)]$		
13	12	8		$F_C[x_{C\|13}(L)] - F_C[x_{C\|12}(L)]$		$F_A[x_{A\|13}(L)] - F_A[x_{A\|15}(L)]$
13	12	4	$F_D[x_{D\|13}(L)] - F_D[x_{D\|12}(L)]$			$F_A[x_{A\|13}(L)] - F_A[x_{A\|15}(L)]$
13	9	8		$F_C[x_{C\|13}(L)] - F_C[x_{C\|15}(L)]$		$F_A[x_{A\|9}(L)] - F_A[x_{A\|13}(L)]$
13	9	1	$F_D[x_{D\|9}(L)] - F_D[x_{D\|13}(L)]$	$F_C[x_{C\|13}(L)] - F_C[x_{C\|15}(L)]$		
13	8			$F_C[x_{C\|13}(L)] - F_C[x_{C\|15}(L)]$		$F_A[x_{A\|13}(L)] - F_A[x_{A\|15}(L)]$
13	5	4	$F_D[x_{D\|13}(L)] - F_D[x_{D\|15}(L)]$			$F_A[x_{A\|5}(L)] - F_A[x_{A\|13}(L)]$
13	5	1	$F_D[x_{D\|13}(L)] - F_D[x_{D\|15}(L)]$	$F_C[x_{C\|5}(L)] - F_C[x_{C\|13}(L)]$		
13	4		$F_D[x_{D\|13}(L)] - F_D[x_{D\|15}(L)]$			$F_A[x_{A\|13}(L)] - F_A[x_{A\|15}(L)]$
13	1		$F_D[x_{D\|13}(L)] - F_D[x_{D\|15}(L)]$	$F_C[x_{C\|13}(L)] - F_C[x_{C\|15}(L)]$		
11	10	8			$F_B[x_{B\|10}(L)] - F_B[x_{B\|11}(L)]$	$F_A[x_{A\|11}(L)] - F_A[x_{A\|15}(L)]$
11	10	2	$F_D[x_{D\|10}(L)] - F_D[x_{D\|11}(L)]$			$F_A[x_{A\|11}(L)] - F_A[x_{A\|15}(L)]$
11	9	8			$F_B[x_{B\|11}(L)] - F_B[x_{B\|15}(L)]$	$F_A[x_{A\|9}(L)] - F_A[x_{A\|11}(L)]$
11	9	1	$F_D[x_{D\|9}(L)] - F_D[x_{D\|11}(L)]$		$F_B[x_{B\|11}(L)] - F_B[x_{B\|15}(L)]$	
11	8				$F_B[x_{B\|11}(L)] - F_B[x_{B\|15}(L)]$	$F_A[x_{A\|11}(L)] - F_A[x_{A\|15}(L)]$
11	3	2	$F_D[x_{D\|11}(L)] - F_D[x_{D\|15}(L)]$			
11	3	1	$F_D[x_{D\|11}(L)] - F_D[x_{D\|15}(L)]$		$F_B[x_{B\|3}(L)] - F_B[x_{B\|11}(L)]$	

11	2		$F_D[x_{D\|11}\ (L)] - F_D[x_{D\|15}\ (L)]$		
11	1		$F_D[x_{D\|11}\ (L)] - F_D[x_{D\|15}\ (L)]$	$F_B[x_{B\|11}\ (L)] - F_B[x_{B\|15}\ (L)]$	
7	6	4		$F_B[x_{B\|6}\ (L)] - F_B[x_{B\|7}\ (L)]$	$F_A[x_{A\|7}\ (L)] - F_A[x_{A\|15}\ (L)]$
7	6	2	$F_C[x_{C\|6}(L)] - F_C[x_{C\|7}\ (L)]$		$F_A[x_{A\|7}\ (L)] - F_A[x_{A\|15}\ (L)]$
7	5	4		$F_B[x_{B\|7}\ (L)] - F_B[x_{B\|15}\ (L)]$	$F_A[x_{A\|5}\ (L)] - F_A[x_{A\|7}\ (L)]$
7	5	1	$F_C[x_{C\|5}(L)] - F_C[x_{C\|7}\ (L)]$	$F_B[x_{B\|7}\ (L)] - F_B[x_{B\|15}\ (L)]$	
7	4			$F_B[x_{B\|7}\ (L)] - F_B[x_{B\|15}\ (L)]$	$F_A[x_{A\|7}\ (L)] - F_A[x_{A\|15}\ (L)]$
7	3	2	$F_C[x_{C\|7}(L)] - F_C[x_{C\|15}\ (L)]$		$F_A[x_{A\|3}\ (L)] - F_A[x_{A\|7}\ (L)]$
7	3	1	$F_C[x_{C\|7}(L)] - F_C[x_{C\|15}\ (L)]$	$F_B[x_{B\|3}\ (L)] - F_B[x_{B\|7}\ (L)]$	
7	2		$F_C[x_{C\|7}(L)] - F_C[x_{C\|15}\ (L)]$		$F_A[x_{A\|7}\ (L)] - F_A[x_{A\|15}\ (L)]$
7	1		$F_C[x_{C\|7}(L)] - F_C[x_{C\|15}\ (L)]$	$F_B[x_{B\|7}\ (L)] - F_B[x_{B\|15}\ (L)]$	

TABLE 7. PROBABILITY OF THREE COMPONENT FAILURE GIVEN TWO COMPONENT FAILED

Failure Sequences	Probability of Failure of Component L ≤ L			
	D	C	B	A
12 8		$F_C[x_{C\|12}(L)] - F_C[x_{C\|14}(L)]$		
12 4	$F_D[x_{D\|12}(L)] - F_D[x_{D\|14}(L)]$			
10 8			$F_B[x_{B\|10}(L)] - F_B[x_{B\|14}(L)]$	
10 2	$F_D[x_{D\|10}(L)] - F_D[x_{D\|14}(L)]$			
6 4			$F_B[x_{B\|6}(L)] - F_B[x_{B\|14}(L)]$	
6 2		$F_C[x_{C\|6}(L)] - F_C[x_{C\|14}(L)]$		
12 8		$F_C[x_{C\|13}(L)] - F_C[x_{C\|12}(L)]$		
12 4	$F_D[x_{D\|13}(L)] - F_D[x_{D\|12}(L)]$			
9 8				$F_A[x_{A\|9}(L)] - F_A[x_{A\|13}(L)]$
9 1	$F_D[x_{D\|9}(L)] - F_D[x_{D\|13}(L)]$			
5 4				$F_A[x_{A\|5}(L)] - F_A[x_{A\|13}(L)]$
5 1		$F_C[x_{C\|5}(L)] - F_C[x_{C\|13}(L)]$		
12 8		$F_C[x_{C\|12}(L)] - F_C[x_{C\|15}(L)]$		
12 4	$F_D[x_{D\|12}(L)] - F_D[x_{D\|15}(L)]$			
10 8			$F_B[x_{B\|10}(L)] - F_B[x_{B\|11}(L)]$	
10 2	$F_D[x_{D\|10}(L)] - F_D[x_{D\|11}(L)]$			
9 8				$F_A[x_{A\|9}(L)] - F_A[x_{A\|11}(L)]$
9 1	$F_D[x_{D\|9}(L)] - F_D[x_{D\|11}(L)]$			
3 2				$F_A[x_{A\|3}(L)] - F_A[x_{A\|11}(L)]$
3 1			$F_B[x_{B\|3}(L)] - F_B[x_{B\|11}(L)]$	$F_A[x_{A\|1}(L)] - F_A[x_{A\|3}(L)]$
10 8			$F_B[x_{B\|10}(L)] - F_B[x_{B\|15}(L)]$	
10 2	$F_D[x_{D\|10}(L)] - F_D[x_{D\|15}(L)]$			

9	8				$F_A[x_{A\|9}\,(L)] - F_A[x_{A\|15}\,(L)]$
9	1	$F_D[x_{D\|9}\,(L)] - F_D[x_{D\|15}\,(L)]$			
6	4			$F_B[x_{B\|6}\,(L)] - F_B[x_{B\|7}\,(L)]$	
6	2		$F_C[x_{C\|6}(L)] - F_C[x_{C\|7}\,(L)]$		
5	4				$F_A[x_{A\|5}\,(L)] - F_A[x_{A\|7}\,(L)]$
5	1		$F_C[x_{C\|5}(L)] - F_C[x_{C\|7}\,(L)]$		
3	2				$F_A[x_{A\|3}\,(L)] - F_A[x_{A\|7}\,(L)]$
3	1			$F_B[x_{B\|3}\,(L)] - F_B[x_{B\|7}\,(L)]$	
6	4			$F_B[x_{B\|6}(L)] - F_B[x_{B\|15}\,(L)]$	
6	2		$F_C[x_{C\|6}(L)] - F_C[x_{C\|15}\,(L)]$		
5	4				$F_A[x_{A\|5}\,(L)] - F_A[x_{A\|15}\,(L)]$
5	1		$F_C[x_{C\|5}(L)] - F_C[x_{C\|15}\,(L)]$		
3	2				$F_A[x_{A\|3}\,(L)] - F_A[x_{A\|15}\,(L)]$
3	1			$F_B[x_{B\|3}(L)] - F_B[x_{B\|15}\,(L)]$	

TABLE 8. FLIGHT LOAD BLOCK

Regime	Rotor Position (Ψ)	Centrifugal Force (lb)	Twist (θ) (degrees)	Bending (ϕ) (degrees)	Cycles
GAG1	0	0	13.5	0	4800
	90	102100	13.5	0.34	
	180	0	13.5	0	
	270	102100	13.5	-0.34	
GAG2	0	0	13.5	0	19200
	90	90980	13.5	0.34	
	180	0	13.5	0	
	270	90980	13.5	-0.34	
Preflight	0	0	0	0	48000
	90	0	-25	0	
	180	0	0	0	
	270	0	28	0	
HSLF	0	65340	0	0	3.8×10^7
	90	65340	-6	0.27	
	180	65340	0	0	
	270	65340	6	-0.27	
Maneuver	0	72040	5	0	7.2×10^6
	90	72040	-5.6	0.3	
	180	72040	5	0	
	270	72040	15.6	-0.3	
Autorotation	0	90980	-12	0	3.7×10^6
	90	90980	-17	0.32	
	180	90980	-12	0	
	270	90980	-7	-0.32	
Limit load	0	102100	28	0.34	na
	90	102100	28	0.34	
	180	102100	28	0.34	
	270	102100	28	0.34	
Ult load 1	0	153150	28	0.54	na
	90	153150	28	0.54	
	180	153150	28	0.54	
	270	153150	28	0.54	
Ult load 2	0	0	0	0	na
	90	0	-75	0	
	180	0	0	0	
	270	0	75	0	

INITIAL DISTRIBUTION LIST

1.	Defense Technical Information Center Cameron Station Alexandria, Virginia 22304-6145	2
2.	Library, Code 0142 Naval Postgraduate School Monterey, California 93943-5002	2
3.	Director, Naval Air Systems Command DET Program Manager Air (Field) - 226 PSC Box 8026 Cherry Point, North Carolina 28533-0026	3
4.	Department of the Navy Naval Air Systems Command Attention: AIR 530A 1421 Jefferson Davis Highway Arlington, Virginia 22243-5300	1